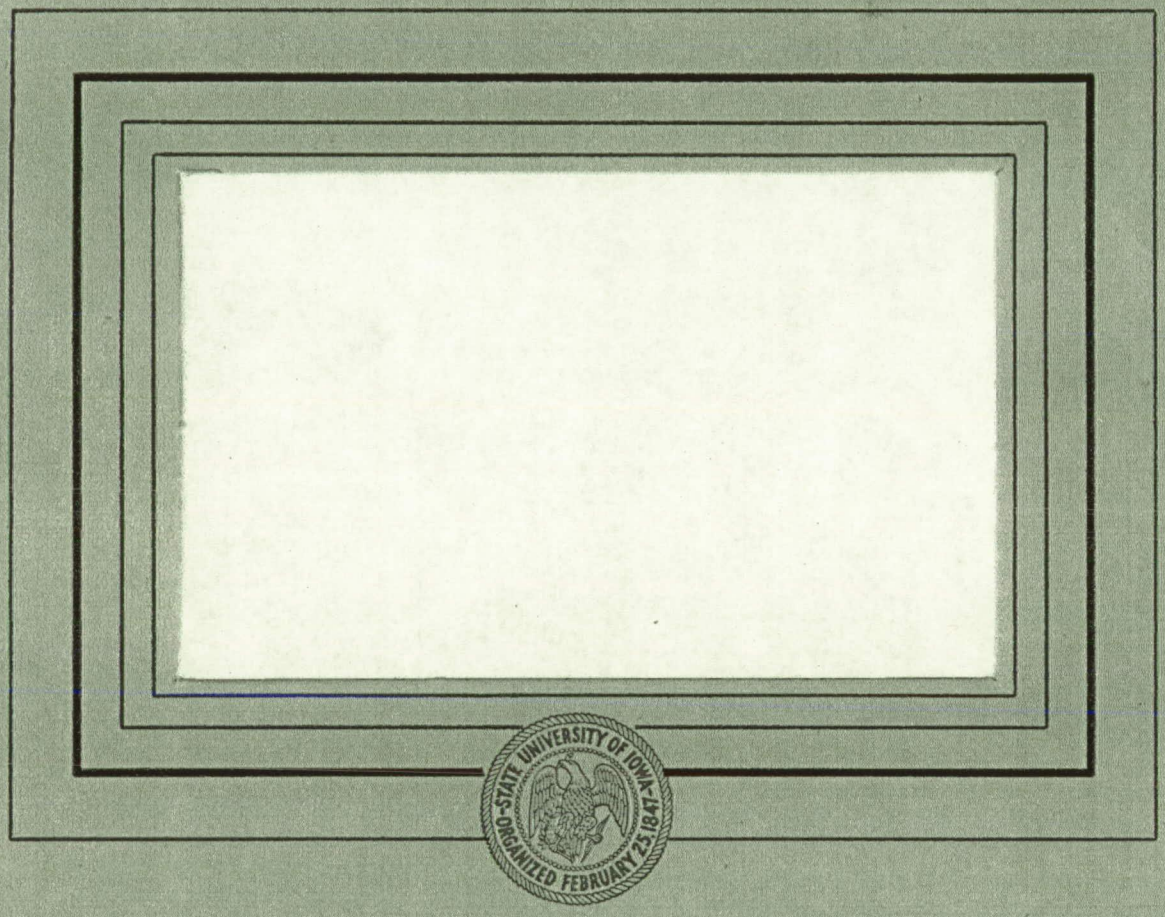

Department of Physics and Astronomy

STATE UNIVERSITY OF IOWA

Iowa City

A SATELLITE BORNE CADMIUM SULFIDE TOTAL CORPUSCULAR ENERGY DETECTOR *

by

John W. Freeman**

A thesis submitted in partial fulfillment of the requirements for the degree of Master of Science in the Department of Physics and Astronomy in the Graduate College of the State University of Iowa

February 1961

Chairman: Professor J. A. Van Allen

* Research assisted by Contract NASw-17 with the National Aeronautics and Space Administration and by Contract N9onr-93803 with the Office of Naval Research (Joint program ONR-AEC).

** Now a Research Fellow of the United States Steel Foundation.

ACKNOWLEDGEMENTS

The author wishes to sincerely thank Drs. James A. Van Allen and Carl E. McIlwain to whom he is indebted for the original suggestions, advice and many helpful discussions. Thanks also are owed to Messrs. Guido Pizzella and James Thissell for stimulating discussions and laboratory assistance, to Dr. George H. Ludwig who oversaw the electronic aspects of the S-46 payload, and to Messrs. Donald Gurnett, William A. Whelpley, Louis A. Frank, Michael Wiemer, William Yeh, Roger Crull and Kay McCune for assistance at various phases of the project. The generous help of Mr. George Carson is acknowledged along with the cooperation of Mr. A. Deuth of the Clairex Corporation. The author also wishes to thank Mrs. Evelyn Robison who typed this manuscript.

TABLE OF CONTENTS

TABLE OF CONTENTS
(continued)

TABLE OF FIGURES

Figure Nos.

TABLE OF FIGURES
(continued)

Page

ABSTRACT

The properties of single crystals of cadmium sulfide as radiation detectors are described. It has been found possible to select crystals such that:

(a) The ratio of increase of conductivity under irradiation to the rate of absorption of energy in the crystal is substantially independent of particle energy (over the examined ranges of 500 ev to 80 kev for electrons and 5 kev to 180 kev for protons) and of the magnitude of energy flux (over the range from .005 to 10 ergs/cm^2-sec); and

(b) The above ratio is substantially the same for protons, electrons, alpha particles, x-rays and γ-rays.

For a driving voltage of 100 volts, typical crystals yield currents of 10^{-7} to 10^{-6} amperes for each erg/cm^2-sec of energy absorbed by the crystal. The threshold of such crystal detectors (resulting from dark currents of the order of 10^{10} amp) is typically 10^{-3} ergs/cm^2-sec. For selected crystals a response-temperature coefficient of -0.25% per degree centigrade is found for the temperature range -50° C to +50° C.

A description is given of a complete CdS total corpuscular energy detector for the study of geomagnetically trapped

radiation by means of a satellite. The detector described has a dynamic range greater than 10^4, a solid angle of 10^{-3} steradian, and a detection threshold of approximately 1 erg/cm^2-sec-sterad. A similar detector employing a small magnet for the selective exclusion of electrons is also described.

Noteworthy practical features of these detectors for satellite and space probe experiments are:

(a) Use of bare crystals, without covering foils, in order to detect charged particles having energies as low as hundreds of electron volts.

(b) Simplicity of electronic auxiliaries.

(c) Compactness, lightweight and nechanical ruggedness.

(d) Low electrical power requirements.

(e) Conversion of conduction current to the rate of a two-state relaxation oscillator in order to facilitate telemetric transmission of data.

A pair of such detectors was flown as part of the S-46 satellite payload on March 23, 1960, but due to vehicular failure an orbit was not achieved and the operation of the CdS detectors was observed for only six minutes of flight.

I. INTRODUCTION

One of the leading instrumental problems associated with the study of the geomagnetically trapped particles is the development of a simple detector capable of responding directly to the great flux of low energy electrons and protons presumably present in the outer radiation zone.[1]

On the basis of preliminary tests in the summer of 1959 Carl McIlwain proposed the investigation of photoconductive crystals as the basis for a new system of detectors. A crystal of photoconductive material such as cadmium sulfide satisfies the criterion of zero wall thickness and is sensitive to photons of a few electron volts energy. The results of an energy sensitivity check looked promising. Hence a systematic investigation into the properties of single crystals of CdS as particle radiation detectors was launched.* It is the purpose of this paper to summarize the results of this investigation.

---

1. Van Allen, J. A., "The Geomagnetically-Trapped Corpuscular Radiation", J. Geophys. Research, 64, 1683-1689 (1959).

* Single crystals of CdS were chosen because they showed a sensitivity to 7 kev electrons several factors of 10 higher than either the sintered CdS or sintered CdSe material. Single crystals of CdSe were not available for examination.

At the time of Dr. McIlwain's suggestion, plans were taking shape for a high apogee satellite, for the study of trapped radiation (payload designation S-46) to be built by the State University of Iowa in cooperation with the Army Ballistic Missile Agency at Huntsville, Alabama (now the George C. Marshall Space Flight Center). It was subsequently agreed that the S-46 payload would include two detectors employing CdS photoconductive crystals* as total-energy charged particle flux meters.

It is an additional purpose of the present paper to describe the design and construction of practical detectors and the calibration procedures which were developed.

---

* The photoconductive crystal chosen was the C1-2 manufactured by the Clairex Corporation of New York. All data in this paper were obtained from crystals of this type.

II. CHARACTERISTICS OF PHOTOCONDUCTIVE CADMIUM SULFIDE CRYSTALS

A. Principles of Operation

It is in general true that every insulator and semiconductor can be made more conductive by the absorption of electron exciting radiation.[2] Certain substances such as CdS, PbS, CdSe, PbTe, PbSe, InSb, Si, and Ge, known as photoconductors, show enhancement of conductivity under irradiation with electromagnetic radiation in or near the visible spectrum. For a number of years the variety of conflicting properties of these semiconductors so baffled investigators that little progress was made in understanding their operation. The new era of solid state physics that has accompanied the advent of the transistor has provided the grounds and language for the understanding of the physical principles of photoconductors. The following discussion is intended to give the basic theory for interpreting the response of photoconductors to ionizing radiation.

---

2. Rose, Albert, "Performance of Photoconductors", in R. G. Breckenridge, B. R. Russell, E. E. Hahn (editors), "Photoconductivity Conference", Section IA, pp. 3-48, John Wiley and Sons, Inc., New York, 1956, page 3.

A portion of the energy level diagram for an electron in a crystal lattice such as that of cadmium sulfide is shown in figure 1. The effect of the regularly spaced neighboring atoms on the potential field experienced by an electron in a given atom is a splitting of the discrete levels into continuous bands. Therefore the band structure represented in the diagram is a result of the periodic atomic potentials. The electronic current, j, in a band is given by the product of the charge of the electron e, and the electron probability current density or,

$$j = \frac{-e\hbar}{2m_e i}\left(\psi^*\nabla\psi - \psi\nabla\psi^*\right) \qquad (1)$$

where ψ is the electronic wave function. As a result of the form of ψ in a periodic potential, the net electronic current in a band (given by the integral of (1) over the entire band) can be shown to vanish for a band completely filled with electrons and to be non-zero for a partially filled band. Therefore, only a partially filled band can carry current under an applied field. The distinction between a conducting crystal and an insulating crystal is now clear. An insulating crystal consists of a material whose outermost electron-containing band is

completely filled, and a conducting crystal a material whose outermost electron-containing band is only partially filled.[3] An unfilled band is referred to as a conduction band. The conduction band may be thought of as an energy state in which an electron can move freely in an applied external field. The transition of a photoconductor from an insulator to a conductor occurs when electrons lying in the filled valence level (or lower levels) absorb energy from incident radiation and are excited into the higher energy level conduction band. In this state the electrons are said to have become free carriers.*

Electrons and holes in the conduction band, however, may fall into potential wells, called traps, which lie in the forbidden zone between the valence and conduction bands. These traps are formed by impurity atoms or other defects of the crystal lattice. Electrons falling into shallow traps (traps close to the conduction band) may re-enter the conduction

---

3. Bube, R. H., "Photoconductivity of Solids", John Wiley and Sons, Inc., New York, 1960, page 31.

* When an electron is excited into the conduction band a hole is left behind. This hole is free to jump from atom to atom and thus an analogous description to that for electrons can be given for holes.

band by virtue of their thermal energy. Electrons falling into deeper lying traps called bound states or ground states may remain there until they recombine with holes and thus end their lives as potential contributors to the photocurrent.

Because of the possibilities of recombination by way of bound states each free carrier has a certain mean lifetime, τ. This mean lifetime refers to the time the free carrier spends in the conduction band and does not include the time spent in shallow traps.*

The lifetime of the free carriers is one of the key factors influencing the conductivity of a semiconductor. The importance of the free carrier lifetime, τ, in determining the response of a photoconductor can be seen by examining the basic equations which apply to the current in a photoconductor. Consider the steady state situation in a given semiconductor. The equation for the current made possible by electron excitation may be assumed to be of the form

---

* The lifetime of a free carrier is not considered to end when a free carrier leaves the semiconductor through an electrode since it is immediately replaced by another of like charge at the opposite electrode.

$$I = e\,G\,N_o \tag{2}$$

where e is the charge of the electron, N_o is the rate of electron excitation in the crystal, and G is a factor containing all other essential parameters.

Assuming Ohm's law,

$$I = \frac{V}{R} = \frac{V_c \sigma A_x}{\ell} \tag{3}$$

where V_c is the voltage applied to the sample, R the resistance of the sample, σ its conductivity, A_x the cross-sectional area, and ℓ the distance between electrodes. If n is the volume density of free carriers (electrons) and μ their mobility in the conduction band, then

$$\sigma = n\,e\,\mu\,. \tag{4}$$

But for the steady state condition the number of free carriers per unit volume in the conduction band must equal n_o, the number excited per unit volume per unit time times their mean lifetime:[4]

---

4. Rose, Albert, "Performance of Photoconductors", in R. G. Breckenridge, B. R. Russell, E. E. Hahn (editors), "Photoconductivity Conference", Section IA, pp. 3-48, John Wiley and Sons, Inc., New York, 1956, page 5.

$$n = n_o \tau . \tag{5}$$

Combining equations (4) and (5) with (3) we have

$$I = \frac{V_c e \mu n_o \tau A_x}{\ell} . \tag{6}$$

Since the average drift velocity is given by

$$\bar{v}_e = \frac{V_c \mu}{\ell} ,$$

we can see that the transit time for a free carrier moving from one electrode to the other is given by

$$T = \frac{\ell^2}{V_c \mu} . \tag{7}$$

Solving for V_c and substituting into equation (6) we have

$$I = e N_o \frac{\tau}{T} . \tag{8}$$

Comparing equations (8) and (2) we see that

$$G = \frac{\tau}{T} . \tag{9}$$

The quantity G, often called the gain factor, is thus the ratio of carrier lifetime to the transit time of a carrier between electrodes. Equation (9) requires no assumptions about the nature of traps. Rewriting equation (2) as

$$G = \frac{I}{e N_o} \tag{10}$$

we note that the gain factor is the ratio of the number of carriers crossing the photoconductor per second, I/e, to the number of excitations in the crystal per second.

It is often convenient to think of the bound states as presenting a certain capture cross section to the free carriers. In terms of the capture cross section, s, the recombination lifetime may be given by,

$$\tau = \frac{1}{v_e s N} \tag{11}$$

where v_e is the velocity of the free carriers and N is the number density of capturing centers.[5]

The process of sensitizing a pure crystal of photoconductive material consists of altering the mean lifetimes of the free carriers by the introduction of new bound states formed by the addition of impurity atoms into the crystal lattice. When either copper or silver is used as an activator for CdS,

---

5. Rose, Albert, "Performance of Photoconductors", in R. G. Breckenridge, B. R. Russell, E. E. Hahn (editors), "Photoconductivity Conference", Section IA, pp. 3-48, John Wiley and Sons, Inc., New York, 1956, page 9.

new bound states which act as hole traps are introduced.[6] The mean lifetime of holes is thus reduced, and as a result the mean lifetime of electrons is increased. Thus electrons become the majority current carriers and the crystal becomes more sensitive to ionizing radiation. For example, in pure CdS both the electron and hole lifetimes are of the order of 10^{-6} seconds whereas in sensitized CdS the majority-carrier lifetime may be as long as 10^{-3} seconds and the minority-carrier lifetime as short as 10^{-8} seconds.[7]

This strong dependence of lifetime on the quantity and relative energy levels of traps brings up one of the most serious difficulties encountered in using photoconductive crystals as detectors of electromagnetic or corpuscular energy over wide dynamic ranges, namely the strong impurity concentration sensitivity of important parameters. Individual crystals from any particular lot may vary greatly in their characteristics. Some may show a linear dependence of current on radiation

---

6. Kittel, Charles, "Introduction to Solid State Physics", John Wiley and Sons, Inc., New York, 1956, page 526.

7. Kittel, Charles, "Introduction to Solid State Physics", John Wiley and Sons, Inc., New York, 1956, page 59.

intensity while others show a sublinear or even superlinear dependence. Furthermore, for a given flux the response of some crystals may change very little with temperature while others become markedly less sensitive with increases in temperature. The absolute sensitivity or gain factor itself may differ from crystal to crystal by several factors of ten. The conclusion is that quantitative statements regarding such characteristics as linearity must be restricted to specific, individual crystals and it should be borne in mind that gross variations of characteristics occur among crystals, even though they are nominally similar.

B. Radiation Sensitivity

1. Definition of Terms

To determine the sensitivity or response of a crystal of CdS to a given flux of a particular type of radiation a completely empirical approach is taken. The crystal conduction current is measured directly under a standard driving voltage. For the purpose of crystal calibration, we adopt the following definition of crystal sensitivity, S,

$$S \equiv \frac{I_c - I_D}{f} \tag{12}$$

where I_c is the crystal current under irradiation, I_D the crystal dark current, both measured in amperes with a driving voltage of 100 volts, and f is the energy flux in ergs per square centimeter per second absorbed in the crystal.

2. Electron Sensitivity

The electron accelerator apparatus used for the determination of CdS crystal sensitivity to electrons is shown diagramatically in figure 2. The transformer-rectifier high voltage power supply is capable of voltages from 2 to 120 kilovolts. The crystal to be irradiated is mounted in the center of a Faraday cup that is used to simultaneously monitor the beam current. The bottom of the Faraday cup is beveled and painted with aquadag to minimize secondary emission. An investigation with a suppressor grid indicated that the cup was satisfactorily designed so that secondary emission produced an error of less than 5% in the beam current measurement.

Measurements with this accelerator showed that it is possible to select Clairex Cl-2 crystals for which the electron sensitivity is nearly independent of particle flux from 10^7 to 10^{10} electrons/cm^2-sec and nearly independent of particle energy

over the range from 2 kev to 80 kev. Mr. G. Pizzella of this laboratory, using a different electron gun, has shown that it is possible to select crystals for which there is no significant change in electron sensitivity down to 500 ev.

For convenient use with experimental data from the apparatus shown in figure 2, equation (12) may be rewritten as

$$S = \frac{(I_c - I_D)\, A}{I_B\, V\, 10^7} \tag{13}$$

where as before I_c and I_D are the measured crystal current and dark current in amperes at V_c = 100 volts, A is the area of the Faraday cup, I_B the total measured beam current, V the accelerating voltage and 10^7 is the conversion factor from joules to ergs.

Typical results obtained with this apparatus are shown in figures 3 and 4. Figure 3 shows data for a crystal whose sensitivity is independent (within experimental error) of beam energy flux over a variation of a factor of 100, using a constant accelerating voltage. Figure 4 shows data for a CdS crystal whose electron sensitivity is substantially independent of particle energy over a range from 2 kev to 80 kev. Since the specific rate of energy loss of an electron in ergs loss per

gram per cm^2 of path, $-(dE/d\xi)$, diminishes by a factor of about 20 from 2 kev to 80 kev,[8] it appears that figure 4 demonstrates that S is independent of $-(dE/d\xi)$. It is, therefore, reasonable to assume that S continues to be independent of particle energy for all higher energies.* The gradual increase in sensitivity evident in figure 4 is characteristic of most of the electron data. For the majority of crystals the slope is greater and in a fewer number of cases may even be negative.

In early measurements major sources of error were electron beam inhomogeneity and instability. Refinements in the electron gun including a grid at cathode potential placed in front of the filament have improved the beam. An additional source of error was the quenching of the crystal photocurrent due to infrared radiation from the hot filament. CdS shows a quenching effect for photons of energy less than the band gap energy due to freeing of trapped holes, making them available for recombination

---

8. Fermi, E. (Orear, Rosenfeld, Scheuter), "Nuclear Physics", University of Chicago Press.

* A typical crystal used in this work has a thickness equivalent to the extrapolated range of a 500 kev electron. Higher energy electrons therefore lose only a portion of their energy in the crystal. But note that the basic definition of S is in terms of <u>energy absorbed</u>.

with electrons.[9] A method of coating the filament that eliminates the problem was found. The efficacy of this measure was demonstrated by comparing the response of the crystal to equivalent white light fluxes from a separate source with the filament on and off.

In practice, the experimental error in the calculated sensitivity is determined by the scatter of observed points if this error exceeds the cumulative apparatus errors. Assuming the manufacturer's stated errors of $\pm$ 2% in both the Keithley and Victoreen electrometers and $\pm$ 5% in the electrostatic voltmeter used to calibrate the high voltage power supply, and taking $\pm$ 5% as the error in the current collecting accuracy of the Faraday cup, the error of the measurements in figures 3 and 4 is $\pm$ 14%. Leakage currents were found to be less than 1% for both beam current and crystal current.

3. Proton Sensitivity

Figure 5 is a graph of CdS crystal sensitivity versus proton energy for protons accelerated by the Iowa Cockcroft-Walton accelerator. The beam current was monitored by means of a Faraday cage mounted on a movable shaft and placed in the exact

---

9. Kittel, Charles, "Introduction to Solid State Physics", John Wiley and Sons, Inc., New York, 1956, page 529.

position of the crystal.* Experimental error is greater here due to inhomogeneity of the beam and difficulty in obtaining a stable beam at sufficiently low intensities. In spite of this the graph shows good grouping of points, with crystal No. 105 showing a sensitivity variation of less than a factor of 3 from 20 to 180 kilovolts and crystal No. 103 showing a variation of approximately a factor of 3 from 5 to 50 kilovolts.

On the basis of more recent data taken with a Texas Nuclear Corp. 150 kilovolt proton accelerator, Mr. Pizzella estimates that it is possible to obtain crystals whose sensitivity varies by less than 30% from 5 to 100 kev proton energy.

Figure 6 shows both proton and electron data for the same crystal plotted on the same graph. Both sets of data show the same order of magnitude of sensitivity. This result has been confirmed for more than 10 other crystals.

As can be seen from figure 5, proton sensitivity tends to decrease with increasing particle energy. This tendency is the opposite of that of electron sensitivity, insofar as it is meaningful to risk a general statement.

---

* Faraday cage apparatus designed by Mr. G. Pizzella.

4. Alpha Particle Sensitivity

The sensitivity of CdS crystals to 5.3 mev alpha particles was measured using a Polonium 210 source. The source strength was calibrated by a mica window geiger tube whose effective counting area had been previously determined. At a point 0.5 cm from the source, the source provided an alpha particle flux of 0.15 ergs/cm^2-sec for calibrating the crystals. Employing this source, Mr. William Yeh has measured the alpha sensitivity of some 30 crystals. Table 1 is a partial list of the results comparing the alpha sensitivity with the electron sensitivity. In nearly every individual case the value of the (energy) sensitivity for alpha particles falls within a factor of 2 of its average value for electrons.

5. X-Ray Sensitivity

Using accurate Victoreen ionization chambers, Louis Frank (Intradepartmental Report 1959) has made a series of calibrations of the x-ray beam from a Westinghouse Quadrocondex. Using identical absorbers and positions, data have been taken on the response of CdS crystals to the x-ray beam.

Table I

COMPARISON OF ALPHA PARTICLE SENSITIVITY AND ELECTRON SENSITIVITY

Crystal No. (Cl-2)	Alpha Sensitivity (amp/erg/cm^2-sec) x 10^{-7}	Average Electron$^+$ Sensitivity (amp/erg/cm^2-sec) x 10^{-7}	$\frac{S_{e\ max}}{S_{e\ min}}$*	$\frac{S_\alpha}{S_e}$**
275	4.4	2.3	1.5	1.9
278	8.8	4.6	2.0	1.9
279	2.6	5.0	3.5	0.52
281	0.28	0.23	1.5	1.2
283	2.8	2.6	1.5	1.1
287	7.2	3.0	1.5	2.4
291	15.4	10.0	2.5	1.5
294	2.7	2.6	2.0	1.04
296	7.5	4.6	1.5	1.6
304	5.9	2.3	3.0	2.5
305	7.8	4.0	2.0	2.0

+ Electron sensitivity averaged over a flux range of 10^7 to 10^9 electrons/cm^2-sec and an energy range of 5 to 80 kev.

* The ratio of the maximum value of the electron sensitivity to the minimum value over the same ranges.

** The ratio of the alpha particle sensitivity to the average electron sensitivity.

Using the relation that one roentgen equals 87 ergs/gm in dry air,[10] and comparing the mass absorption coefficient of CdS with that of air we can arrive at an estimate of the x-ray energy flux absorbed in the crystal.

To simplify estimates of the mass absorption coefficient and the x-ray beam energy spectrum, absorbers consisting of 0.5 inches of yellow brass and 0.021 inches of sheet steel were used with high beam voltages. The x-ray gun tungsten target has the K_{α_1} edge at 60 kilovolts; thus with the brass and steel absorbers and a voltage setting of 170 kilovolts and the x-ray spectrum lies mainly between 100 kv and 170 kv (L. Frank, private communication).

Since the mass absorption coefficients for cadmium and sulfur are not given in tables as a continuous function of energy, it is necessary to pick a wavelength for which they are known and try to obtain a spectrum that has this wavelength as a good approximation. This is an acceptable procedure since the K edge of cadmium is 27 kv and hence the mass absorption coefficient is not a rapidly varying function of x-ray energy in the

---

10. American Institute of Physics Handbook, McGraw-Hill, New York, 1957, pp. 8-251.

region 100 kv to 170 kv. S. J. M. Allen gives 1.09 and 0.166 cm^2/gm for the mass absorption coefficients of cadmium and sulfur respectively for x-rays of wavelength corresponding to 127 kev.[11] If we let 127 kev be representative of our 100-170 kilovolt spectrum the mass absorption coefficient of CdS is approximately 0.9 cm^2/gm. For 100 kev the mass absorption coefficient of air is 0.155.[12] The x-ray energy absorbed by the crystal in erg/gm-sec is then given by the product of the beam flux in R/hr, 87/3600 and the ratio of the mass absorption coefficient of CdS to that of air. Values for the x-ray sensitivity obtained in this manner agree with values for the sensitivity determined by methods previously discussed.

The x-ray beam also provides a convenient source for checking crystal response linearity by changing the distance of the crystal from the x-ray target. Figure 7 shows the response of a detector versus the beam intensity for a constant x-ray energy.

---

11. Compton, A. H., and Allison, S. K., X-Rays in Theory and Experiment, D. Van Nostrand Co., 1955, Appendix IX.

12. McGinnies, R. T., X-Ray Attenuation Coefficients from 10 kev to 100 Mev, National Bureau of Standards Circular 583 Supplement.

6. Temperature Effect on Sensitivity

The effect of temperature on the sensitivity of CdS crystals was measured during irradiation by beta particles and by light sources. Figure 8 shows the response of four crystals as a function of temperature to beta particles from a 1 millicurie Tl^{204} source. For selected crystals a typical variation in sensitivity is -0.25% per degree centigrade from -50° C to +50° C. All such measurements were made at a pressure of 25 mm of Hg to reduce moisture condensation on the crystals. When the sensitivity is defined as in equation (12) the thermal variation of the dark current does not affect the temperature coefficient of S.

7. Maximum Tolerable Radiation Flux

For a particle beam flux exceeding 10 ergs/cm^2-sec a peculiar effect is noted: viz., the response time of the CdS crystal is radically lengthened such that upon removal of the radiation, the photocurrent remains at the level prevailing during the irradiation. Days are required for the crystal to return to the normal dark current condition. The effect exhibits a gradual onset with slight increases in the response time be-

coming apparent at fluxes as low as approximately 5 ergs/cm^2-sec.

The effect has been observed for both electrons and protons but not for x-rays or light at comparable energy fluxes.

To date there is no satisfactory theoretical explanation for the effect. Surface heating is ruled out by the fact that the joule heating for the induced current is several factors of ten greater than the heating due to particle energy loss and yet the effect persists when there is no applied electric field during the irradiation. Electrons of energy for which the effect is observed (as low as 3 kev) are not individually capable of transferring enough energy to the crystal atoms to remove them from the lattice. This is not true for protons, however.

In practice the problem is evaded by the use of a geometric factor which limits the anticipated maximum radiation flux to less than 10 ergs/cm^2-sec.

8. Consistency of Observed Sensitivities and Accepted Values for Mean Lifetime

By the data thus far presented it has been established that sensitized single crystals of CdS can be selected that have an intrinsic radiation sensitivity that is nearly independent of particle energy and mass. This sensitivity is found to be

typically 10^{-7} to 10^{-6} amp/erg/cm^2-sec.* Combining equation (9) with equation (10) we have

$$\frac{\tau}{T} = \frac{I_C}{e N_o} . \tag{14}$$

Solving equation (12) for I_C and substituting in equation (14) (neglecting the usually much smaller dark current), we have,

$$\tau = \frac{T S f}{e N_o} . \tag{15}$$

Or by equation (7)

$$\tau = \frac{\ell^2 S f}{V_C \mu e N_o} . \tag{16}$$

The number of exited carriers introduced into the crystal conduction band per second may be approximated by

$$N_o = \frac{f A_C 6.2 \times 10^{13}}{E_{B.G.}} \tag{17}$$

where f is, as before, the energy flux in ergs/cm^2-sec, A_C is the area of the crystal, $E_{B.G.}$ is the band gap energy in ev and 6.2×10^{13} is the conversion factor from ergs to ev. Thus,

---

* At 100 volts crystal voltage.

$$\tau = \frac{\ell^2 \, S \, E_{B.G.}}{V \mu e \, A_C \, 6.2 \times 10^{13}} \, . \qquad (18)$$

We have an expression for the majority carrier lifetime in terms of the measured sensitivity. With the following values:

$S = 10^{-6}$ amp/erg/cm^2-sec

$\ell = 0.2$ cm

$E_{B.G.} = 2.4$ ev

$V_C = 100$ volts

$\mu = 200$ cm^2/volt-sec [13]

$e = 1.6 \times 10^{-19}$ coul

$A_C = 0.02$ cm^2

we have $\tau \tilde{=} 10^{-3}$ seconds. Bube and others give 10^{-3} seconds as a typical majority carrier lifetime in sensitized CdS.[14] Hence, our values for sensitivity yield lifetimes which are in good agreement with those of other researchers.

---

13. Bube, R. H., "Photoconductivity of Solids", John Wiley and Sons, Inc., New York, 1960, page 269.

14. Bube, R. H., "Photoconductivity of Solids", John Wiley and Sons, Inc., New York, 1960, page 59; and
Rose, Albert, "Performance of Photoconductors", in R. G. Breckenridge, B. R. Russell, E. E. Helm (editors), "Photoconductivity Conference", Section IA, pp. 3-48, John Wiley and Sons, Inc., New York, 1956, page 11.

C. Response Time

The following factors determine how closely the photoconductor signal follows time variations in the incident flux:

(1) Initial flux value.

(2) Final flux value.

(3) Time rate of change of flux.

(4) Previous irradiation history.

(5) Temperature.

Dealing first with item (3), let us choose the case that is most easy to examine experimentally and which is the most severe from the standpoint of the signal misrepresenting the actual flux, namely a step function change in incident flux. The response time can be defined as the time required for the crystal current to come within 10% of the final asymptotic value following a stepwise change in incident flux.

Further, assume that the flux value previous to the change has remained unchanged for a period which is long compared with the response time. This requirement eliminates item (4) as a significant factor.

Regarding final flux values, two distinct physical processes govern the response time. For high final flux values

the response time approaches the free carrier lifetime. For low final flux values thermally re-excited electrons from shallow traps lengthen the response time by several factors of ten (an analogous situation to after-glow in a phosphor). Different experimental and mathematical techniques are required to handle the two regions of the dynamic range in which each of these processes dominates.

Consider first the high flux, fast response time region which begins approximately at crystal currents 100 times dark current. The response times are fast enough that they can be conveniently measured with an oscilloscope. Figure 9 is a schematic diagram of the circuit. Figure 10 is a series of photos taken of oscilloscope traces showing the rise and fall of the crystal current (upper beam) and the corresponding change in glow tube current (lower beam). It is immediately evident that the rise and fall response times increase with decreasing light levels. This is shown graphically over a wider dynamic range in figure 11. Figure 11 also shows the influence of temperature on high and moderate current response time, i.e., lower temperatures mean larger response times. We conclude that response times for which the initial or final current lies in the high to moderate range (approximately 10^{-5} to 10^{-8} amp) can

readily be measured for each crystal, and in general, response times in this class generated by a stepwise change in radiation flux (in itself a worst case) are short enough to be ignored on a time scale of satellite events.

For low radiation fluxes (less than approximately 100 times dark current) the response times lengthen greatly. Figure 12 shows a typical crystal response* as a function of time following the complete removal of low level incident radiation at time $t = 1$ second. The response is described by

$$\log I_C = \log C + \alpha \log t \qquad (19)$$

where C is a constant, t the time and α the slope of the curve on a log-log plot. The constant α is less than 1 in absolute magnitude and increases numerically with increase in initial current. A similar power law is exhibited for the current rise following a sudden radiation increase. α is observed to vary by approximately 10% from 0° C to +50° C.

---

* Here the crystal analog current has been converted linearly to a frequency in a manner to be described in section IIIA 2.

D. Dark Current

Following irradiation most of the crystal current is due to thermally re-excited electrons from shallow traps. Eventually a current value characteristic of the crystal's temperature is approached asymptotically. This zero-irradiation current is called the dark current and varies approximately as the seventeenth power of the absolute temperature for a crystal voltage of 100 volts. For room temperature the dark current of selected crystals lies between 10^{-9} and 10^{-10} amp.

E. Temporal Stability

Over a period of one month a Cl-2 was irradiated continuously with a Thallium 204 beta source (approximately 0.5 ergs/cm^2-sec). During this period there was no change within the accuracy of the electrometer in the crystal response, the dark current or response time.

III. DETAILS OF THE DETECTOR

The following is a description of the two total corpuscular energy detectors employing CdS crystals used on the S-46 payload.

A. The Clairex Cl-2 Crystal Mounting

The S-46 detectors employed the Clairex Cl-2 which is a single crystal of CdS mounted on a ceramic disc 1/4 inch in diameter. A cylindrical lucite encapsilant 1/2 inch long and 1/4 inch in diameter supports the disc and the wire leads. The electrodes are indium and solder. The crystals are typically 2 mm x 2 mm and vary in thickness from 0.5 mm to 0.2 mm.

B. Mounting Details and Characteristics of the Detector

Figure 13 is a diagram showing a cross section of the detector. The crystal itself is mounted in an open-end lead casket (wall thickness = 2 gm/cm^2) and looks out through the solid angle defining aperture and a series of light baffles.

1. Geometric Factor

By the definition we have adopted for sensitivity the effective area of the crystal itself becomes one of the

parameters determining S and hence the usual equation for the effective geometric factor, G,

$$G = \Omega A \tag{20}$$

where A is the effective area of the detector and Ω the solid angle, reduces to

$$G = \Omega . \tag{21}$$

For a unidirectional energy flux, F, in ergs/cm^2-ster-sec, we write

$$F\,\Omega = f = \frac{I_C - I_D}{S} \simeq \frac{I_C}{S}$$

$$\text{or} \qquad F = \frac{I_C}{\Omega\, S} \tag{22}$$

where the approximation sign holds when the crystal current due to radiation is well above the dark current. Thus the unidirectional energy flux sensed by the detector is merely the crystal current divided by the product of the detector solid angle and the crystal sensitivity.

Ω is chosen on the basis of an estimate of the maximum anticipated energy flux, F_{max}. To avoid the damage effect described in the previous section we choose Ω such that

$$f_{max} = 10 \text{ ergs/cm}^2\text{-sec}.$$

On the assumption that F_{max} for geomagnetically trapped radiation is 10^4 ergs/cm^2-ster-sec, Ω becomes 10^{-3} steradians.* The solid angle is defined by an aperture 0.107 cm in diameter and 3 cm from the crystal, so that Ω is 10^{-3} ster.

In order to compute the opening angle corresponding to this solid angle it is necessary to adopt a value for the effective diameter of the irregular shaped crystal. A typical value of 0.2 cm yields a total opening angle of approximately 6 degrees.

2. Dynamic Range

Having chosen Ω, the dynamic range of the detector is determined by the sensitivity, the dark current and the maximum

---

* This estimate of F_{max} is derived from a comparison of the particle energy density and the energy density of the magnetic field

$$\mathcal{E} = \frac{H^2}{8\pi}.$$

The estimate includes an assumption of trapped electron velocity of 10^{10} cm/sec and a maximum outer zone trapping field strength of 0.02 gauss.

current through equation (22). For a crystal of sensitivity 10^{-7} amp/erg/cm^2-sec and dark current 10^{-10} amp,

$$F_{min} = 1 \text{ erg/cm}^2\text{-ster-sec.}$$

The maximum current is set by a 10 megohm precision resistor at 10^{-5} amp. Therefore,

$$F_{max} = 10^5 \text{ erg/cm}^2\text{-ster-sec.}$$

3. Effectiveness of Light Baffles

The CdS crystal being sensitive to visible and ultraviolet light, steps must be taken to avoid stimulation of the detector by sunlight, moonlight and earth light when these light sources lie outside the opening angle of the detector. A series of knife-edge light baffles designed to minimize reflection into the crystal by multiple reflection serves this purpose. The edge of each baffle aperture is set successively farther back from the line of sight of the opening angle. The interior of each baffle is coated with Kodak black brushing lacquer.

A 500 watt slide projector is used to simulate the sun to test the effectiveness of the light baffle system. Photo-

metric measurements indicate that the 500 watt projector is approximately 1/2 as bright as the sun when used at one foot. Figure 14 is a graph showing the detector response to the projector as a function of the angle between the axis of the light beam and the longitudinal axis of the detector. At an angle of 15° off the axis of the detector the projector produces a detector response of approximately 5 times the dark current.

Recent satellite experiments designed around the CdS detector include an optical monitor that is identical to the particle detectors except for a 2 mm quartz window.

4. The "Broom" Magnet

The S-46 scientific payload employed two CdS detectors. The first was open to particles of all energies. The second employed a small permanent magnet to sweep electrons of energy less than 500 kev out of the line of sight of the detecting element. Figure 15 shows the position of the magnet in the detector assembly. The magnet used was a disc type (magnetized along a diameter) with a 1/4 inch hole in the center. A grooved aluminum insert was placed in the gap to prevent electrons from scattering back into the crystal.

Calibration of the cutoff energy was accomplished by mounting a 1 millicurie Thallium 204 beta source in front of the detector and replacing the CdS crystal with a mica window geiger tube of approximately the same effective area. The tube used, an Anton 223, is capable of detecting electrons of energy as low as 30 kev. Thallium 204 has a maximum energy of 760 kev and an average energy of approximately 250 kev. Counting rates with and without the magnet were recorded and a numerical integration under the theoretical spectral curve gave the cutoff energy of the magnet. Background runs showed that the effects of cosmic rays and bremsstrahlung from the source were negligible.

Cutoff energies of very close to 500 kev were found for the magnets of both S-46 flight units. Based on the difference in data obtained from run to run we can estimate the error in this measurement to be $\pm$ 50 kev. The irregular shape of the crystals and imperfect centering of the crystal on the ceramic disc are in a large measure responsible for the inaccuracy in the measurement.

The magnetic field strength along the longitudinal axis of the detector was measured with a Hall effect magnetometer. Calculations of the theoretical cutoff using these measurements

depends strongly on small angles which are difficult to measure accurately but in general agreement is within experimental and calculational error.

A cutoff energy of 500 kev for electrons corresponds to 400 ev for protons. At 500 kev, electrons are nearly penetrating the average crystal so their contribution to crystal ionization is decreasing. Thus one has a detector which is sensitive with decreasing efficiency to electrons above 500 kev but which responds to protons above 400 ev. The average crystal thickness is equivalent to the range of a 10 mev proton.

Improved magnet designs for recent detectors have yielded similar magnets which have cutoff energies for electrons above 600 kev and yet have stray fields of less than 1 γ at 1 meter ($1\ \gamma = 10^{-5}$ gauss).

5. Detector Response to Bremsstrahlung

Electron bombardment of the satellite shell results in the production of x-rays. To minimize the response to these x-rays the CdS crystal is mounted in a lead casket whose wall thickness is 2 gm/cm^2. In addition a 2 gm/cm^2 lead disc is mounted immediately behind the solid angle defining aperture

(see figures 13 and 15).

The effective solid angle for the x-rays is 4π steradians while that for the electrons which produce them is 10^{-3} steradians. The efficiency of conversion of electron energy to x-ray energy of all frequencies is given by

$$\epsilon = a' Z (V + 16.3 Z)$$

where a' is $1.2 \pm 0.1 \times 10^{-9}$, z is the atomic number of the target, and V is the electron voltage.[15] For a simple-minded estimate, irradiation of the equipment by an isotropic 100 kev electron beam is assumed. For 100 kev electrons producing bremsstrahlung on the aluminum wall of the satellite, $\epsilon = 1.5 \times 10^{-3}$. An effective absorption coefficient for the x-rays thus produced is taken to be 5 cm^2/gm. The corresponding attenuation factor in 2 gm/cm^2 of lead is 5×10^{-5}.

Hence the ratio of the electron energy flux reaching the crystal through the entrance aperture to the x-ray energy flux reaching the crystal from 4π steradians is of the order of 10^3; and since the electron energy is wholly absorbed whereas the

---

15. "Handbook of Physics", E. U. Condon and H. Odishaw, editors: Chapter 8, X-Rays, E. U. Condon, McGraw-Hill Book Company, New York, 1958.

x-ray energy is only partially absorbed by the crystal it appears that the detector's output will contain a negligible contribution from the x-ray irradiation which accompanies the electron beam.

An experimental test of this estimate was made by first irradiating a bare CdS crystal with a laboratory x-ray beam (100 - 200 kev), then irradiating a complete detector containing the same crystal with the same x-ray beam. The observed reduction in crystal response by the shielding of the detector assembly was by a factor of about 30 (far less than the idealized estimate of 2×10^4). The discrepancy is apparently due to multiple scattering of x-rays and secondary electrons in the imperfectly shielded system. Nonetheless, it appears that with the S-46 detectors, having a solid angle of 10^{-3} steradian, the direct electron contribution will probably exceed the x-ray contribution by an order of magnitude for actual outer zone conditions. Future detectors should be critically examined for the efficacy of the shielding in order to improve this ratio.

C. Associated Electronics

1. Conversion of Crystal Current to Pulse Form

The current resulting from the change in conductivity of the crystal is readily converted to pulse code modulation form for ease of data handling. The conversion is performed by a simple neon glow tube relaxation oscillator (after a method by Vernov, et al.[16] for monitoring photomultiplier tube anode currents). Figure 16 is a schematic of the circuit including the pulse amplifier. Current through the crystal determines the charging rate of the capacitor and hence the firing rate of the neon tube. Pulses from a voltage divider in the discharge path are inverted and shaped by a saturating bootstrap amplifier used to drive a 9 stage set of binaries.

As shown by figure 17, the frequency of the relaxation oscillator is proportional to the crystal current over a dynamic range of greater than 10^4. Hence one can write

$$I_C = K \nu \qquad (23)$$

---

16. Vernov, S. N., Special Lecture, Fifth General Assembly of C.S.A.G.I., Moscow, July 30-August 9, 1958.

where ν is the frequency of the relaxation oscillator, or detector frequency, and K is the proportionality constant. Combining this with the defining equation for sensitivity we have

$$f = \frac{K\nu}{S} \tag{24}$$

where f is, as before, the particle energy flux. f is found from the energy flux F in ergs/cm^2-ster-sec by $F\,\Omega = f$. Therefore we write

$$F = \phi\,(F)\,\nu \tag{25}$$

by defining

$$\phi \equiv \frac{K\,(I_C)}{\Omega\,S\,(I_C)} \cdot \tag{26}$$

K is typically 10^{-7} ampere-seconds. For a detector with an average electron-proton sensitivity of 10^{-7} amp/erg/cm^2-sec and an Ω of 10^{-3} steradians, equation (25) becomes

$$F = 10^3\,\nu$$

which provides a convenient rule of thumb for approximate conversion from detector output frequency to total energy flux.

In a more realistic case, as we have already seen, S is not a constant but a quantity which can be tabulated as a function of energy flux, f (i.e. I_C). (Crystals are selected so that S is as nearly independent of particle kinetic energy as possible. Any dependence which exists must be neglected since the particle energy spectrum is unknown.) The calibration curve for the current to frequency converter may not be exactly linear but in any event yields $K(I_C)$. Therefore from S (f) or equivalently $S(I_C)$ and $K(I_C)$ we can obtain $\phi(f)$ and hence $\phi(F)$. From equation (25) F vs ν can be graphed. Figure 18 is such a graph for one of the S-46 flight unit detectors. For the case illustrated the graph of equation (25) is seen to take the form

$$F = \phi \nu^{\beta} \tag{25a}$$

where ϕ may now be thought of as a constant whose energy dependence has been replaced by the power law ν^{β}. Here ϕ is 10^3 and β is 0.83. The result is a detector calibration law which lends itself to rapid conversion from data to energy flux.

It was found that the dynamic range of the current to frequency converter was optimum when General Electric Ne 81's

or Ne 76's were used as the neon discharge tubes and Corning glass capacitors were used as the charging capacitor. Carefully selected Ne 81's or Ne 76's are quite temperature stable. The frequency produced for a given input current for selected tubes varies less than 0.05% per degree centigrade between + 50° C and - 50° C.

Proper performance of the relaxation oscillator circuit at low currents requires that leakage current across the capacitor be as low as possible. During testing, the discharge tubes must be isolated from light and the relative humidity must be kept low. During the actual construction of the circuits all parts must be thoroughly cleaned and there can be no epoxy resin or encapsilant film forming a path between the high and low impedance points since an insulation resistance of the order of 10^{13} ohms is required. The glass capacitor must be selected for low leakage current.

The size of the capacitor determines the value of K. This can be chosen to fit the telemetry system parameters. In the case of S-46 (continuous telemetry on all channels) the capacitor was chosen to give a maximum frequency of 0.2 cps after a scaling factor of 512. Thus the saturation current of 10^{-5} amp (determined by a 10 megohm precision current limiting

resistor in series with the crystal) produced a frequency of approximately 100 cps and the crystal dark current corresponded to a time between pulses of greater than 100 seconds. The capacitor chosen was approximately 4300 $\mu\mu f$ d but depended on the firing voltage of the neon tube. Circuits using smaller capacitors have a lower "threshold-of-operation current", presumably because of the lower leakage current.

2. Power Supply, Pulse Shaping Amplifier, and Scalers

See figures 17 and 19.

The power supply, pulse shaping amplifiers and scalars used with the CdS detectors on S-46 have been extensively described by G. H. Ludwig in his doctorate dissertation.[17] Briefly, the positive 6 volt pulse from the glow tube discharge drives a saturating bootstrap amplifier utilizing 2 silicon NPN (2N338) and 1 silicon PNP (2N329A) transistors. The output of the amplifier is a negative pulse, Zener-diode-clipped at 3.1 volts. The pulse duration is approximately 20 μ sec. The pulse is next fed to a series of 9 base driven scalars employing

---

17. Ludwig, G. H., "The Development of a Corpuscular Radiation Experiment for an Earth Satellite", Ph.D. dissertation, State University of Iowa (August 1960).

2N338 transistors. A logic circuit which mixes the outputs of the 1st, 5th and 9th scalars shifts the output base voltage by a different amount with changes of state at each of these three scalars. Integration of the resulting waveform results in a system of low information rate and wide dynamic range, allowing a minimum receiver bandwidth. This system was used with success on Pioneers III and IV.

The 160 volt power supply (see figure 19) is a transistor D.C. to D.C. converter employing Zener Diode regulation.

Table II gives the power and weight specifications of the 2 CdS detectors used on payload S-46.

D. Procedure and Criteria for Selection of Components

The following is an outline of the procedure for selection of components for the S-46 CdS detectors.

1. CdS Crystals

(a) Dark Current. The dark current of each crystal is recorded and plotted as a function of time following saturation with a 100 watt bulb at 1 foot. Crystals with currents less than 10^{-9} amp after 10 min. are considered suitable for further testing.

Table II

S-46 CdS DETECTOR ELECTRICAL AND WEIGHT SPECIFICATIONS

Detector	Power (mw)		Weight (gms)	Stray Magnetic Field (γ at 1 meter)
	Pulse Amplifier + 6 volts	160 Volt Power Supply		
A	0.04	2.0	230	1.5
B	0.04	2.0	175	1.0

This test serves as a relative response time check.

(b) Mechanical. The epoxy and plastic encapsilation material are removed, exposing the bare crystal. A visual inspection is performed. Any sign of crystal breakage or electrode imperfection is cause for rejection.

(c) Temperature Cycle. Using a 1 mc, Tl^{204} beta source to stimulate the crystals to approximately 100 times dark current, the variation of crystal response with temperature is recorded. A crystal whose response varies by more than a factor of 2 from + 75° C to - 50°C is rejected from flight use. The cycle during which the data are taken is preceded by 3 temperature cycles over the same range. This test is performed in vacuo to insure against moisture condensation on the crystal surface.

(d) Electron Sensitivity. As a preliminary relative electron sensitivity check, the crystals are placed in a jig that holds them a standard distance (1.5 cm) from the Thallium source. Crystals showing an abnormally low response are rejected. (This test is usually performed simultaneously with the temperature test.)

Surviving crystals are then irradiated with the electron accelerator previously described. Crystal electron

sensitivity is graphed as a function of particle voltage and flux. Crystals are selected first on the basis of constant sensitivity vs. voltage. A ratio of $S_{max}/S_{min} = 2$ for electron energies from 5 kev to 80 kev is allowed.

The criterion of constant sensitivity with total energy flux depends on the number of surviving crystals and the time schedule for the payload in preparation. From this point calibrations proceed as described in Section II.

The percentage of crystals found acceptable for flight use is approximately 10% of the crystals started through the testing program.

2. Neon Discharge Tubes

(a) Initial Leakage Test. The D.C. resistance of the neon discharge tubes is measured at 60 volts (12 volts below firing voltage) with the tubes in total darkness. Tubes with D.C. resistance of less than 5×10^{10} ohms are rejected.

(b) Firing Voltage Stability. The neon tubes are placed in a circuit identical to that in which they are to be used. The variation in the firing voltage is measured by the variation in height of the voltage pulses taken from the pulse

forming resistors. An average variation of $\pm$ 0.5 volts is tolerated. This variation is measured for a fixed set of currents covering the useful dynamic range.

(c) Frequency - versus - Current Linearity and Low Current Operation. The frequency - versus - current curve is obtained and tubes showing marked deviations from linearity are rejected. The tubes are checked for proper pulsing with a charging current of 10^{-10} amps.

(d) Matching. Following this the tubes are matched with the capacitors to give the desired maximum pulse rate, and the circuits are constructed.

(e) Temperature Test. Current versus frequency curves are obtained for temperatures at 25° C intervals from + 75° C to - 50° C. A variation of 10% in the frequency for a given current (the lower currents are more temperature sensitive) is the maximum allowed. This criterion is not difficult to meet. This test serves as a temperature calibration of the current to frequency converter. This test is performed in vacuo.

(f) Low Current Threshold of Operation. After the flight circuits have been chosen, the current-operation threshold is determined by the use of high value resistors. This enables one

to match the best circuits to the crystals with the lowest dark current.

3. Pulse Shaping Amplifiers

(a) Temperature Test. After aging and testing of the components the bootstrap amplifiers are assembled and temperature cycled 5 times between - 50° C and + 75° C. On the 6th temperature cycle data are taken at 25° C intervals on the following items:

(1) Pulse height ($\simeq$ 3.1 volts).

(2) Pulse rise time ($< 2\ \mu$sec).

(3) Pulse width at half height ($\simeq 15\ \mu$ sec).

These quantities must show no change and must have the values given.

E. Miscellaneous

1. Optical Sensitivity of the Detectors and Response to Heavenly Bodies

The optical sensitivity of the CdS crystals chosen for flight is obtained for the green light from phosphorous excited

by a radioactive tritium source.* For simplicity in determining the light sensitivity we relax our requirement that the f in equation (12) refer to the energy absorbed by the crystal. Let f now be the incident light flux in ergs/cm^2-sec. Light sensitivity as so defined is found to be lower than charged particle sensitivity by a factor between 2 and 10. Presumably this is due to the partial translucence of the crystal. Light sensitivity is strongly spectral dependent with the response rising sharply near the band gap energy, 5100 Å.

Moon:

According to Sears[18], full moonlight provides a light flux of 0.2 lumens/m^2 at the bottom of the atmosphere. This is approximately 0.5 ergs/cm^2-sec which lies in the upper two-thirds of the dynamic range of the detector. This estimate is borne out by actual measurement.

---

* A calibrated light source of this type was purchased from the U. S. Radium Corp. It has a surface luminosity of 1000 microlamberts.

18. Sears and Zemansky, University Physics, Addison Wesley Publishing Co., 1953.

Starlight:

The energy flux of starlight at the earth[19] is about 0.003 ergs/cm^2-sec. This is a factor of 10^3 below the energy detection threshold.

Earthlight:

Allen[20] gives the reflectivity of the earth as 0.34. Also according to Allen, the total solar flux received outside the earth's atmosphere at the mean earth-sun distance is 1.4×10^6 erg/cm^2-sec. The reflected portion of this 0.5×10^6 erg/cm^2-sec is more than enough to saturate the detectors.

Moonlight Reflected from the Earth:

If we assume the moon to be a flat disc receiving 1.4×10^6 erg/cm^2-sec of light radiation from the sun, use 0.07 as the reflectivity of the moon[20] and take the moon to be a point source we find the moonlight flux above the atmosphere

---

19. Orear, Jay, "Fundamental Physics", John Wiley and Sons, Inc., 1960, page 331.

20. Allen, C. W., "Astrophysical Quantities", The Athlone Press, page 231.

to be 0.76 ergs/cm^2-sec (note that since the reflectivity of the earth is 0.34, the transmitted light is 66% of this or 0.5 ergs/cm^2-sec in good agreement with Sear's number). With each square cm of the earth reflecting 34% of 0.76 erg per second moonlight reflecting from the earth will be visible to the satellite borne detector during a full moon.

Aurorae:

Based on figures given by Seaton[21], the directional intensity of visible light from a bright (Class III) aurora is of the order of 0.1 erg/cm^2 sec sterad, a value considerably below the threshold of the S-46 detectors. Hence, it is possible for the detectors to look on an aurora and "see" the particles but not the light.

2. Field Calibration Sources

Field calibrations can be made with radioactive light, gamma, alpha or beta sources. Such sources can be mounted on thin rods and inserted through the aperture of the detectors. A 0.5 mc Co^{60} source a few centimeters from a crystal provides a

---

21. Seaton, M. J., Journal of Atmospheric and Terrestrial Physics, Vol. 4 (1954), pp. 285-294.

detectable current at room temperature. Radioactive light sources are the simplest. The gaseous tritium source (employing a green phosphor) described in the previous section is capable of stimulating detector response to a factor of ten above dark current. Other light sources that have been used are argon glow lamps in conjunction with a constant current generator, electroluminescent panels with a constant voltage source, and tungsten filament lamps with resistance bridges to maintain a uniform filament temperature independent of surroundings. The effects of infra-red quenching should be borne in mind when using a hot filament light source as an absolute calibration standard.

IV. FLIGHT DATA

On the 23rd of March 1960, an unsuccessful attempt was made to place the S-46 trapped radiation study package in orbit.[17] During the 500 second lifetime of the payload following launch, data received from the several tracking stations indicated the satisfactory operation of the two CdS detectors and in fact the entire scientific payload.

The maximum altitude reached during the brief flight (approximately 370 km) was not sufficient to provide particle excitation from the inner belt. The response of the detectors shown in figure 20* is primarily due to optical excitation of the crystals by light from the sunlit earth and the lateral thrust rocket used to push the shroud aside after separation. These data proved helpful in the analysis of payload orientation and malfunction during injection. The detailed correlation of the detector response with the time sequence of injection events has been given by G. H. Ludwig (Ph.D. Dissertation 1960) and hence will be omitted here.

There is, however, a small segment of detector response (1342/55 Z to 1343/09Z) just prior to second stage ignition which cannot be accounted for by optical excitation. It has been

---

* Courtesy of G. H. Ludwig.

suggested by C. E. McIlwain (private communication) that satellite linear motion coupled with the de-excitation of ionospheric oxygen and nitrogen ions might provide a significant energy contribution to the CdS response. Ionized oxygen and nitrogen atoms and molecules may bombard the crystal and in so doing de-excite with the emission of a photon of typically 10 ev. The photon thus emitted would be capable of exciting photoconductivity in the crystal. If one assumes an ion density at payload altitudes[22] of 5×10^5 ions/cm^3 and a final payload velocity of 10 kilometers/sec, then ions can deliver energy to the CdS detectors which look in the direction of motion at the rate of 1 erg/cm^2-sec at fourth stage burnout. At booster burnout the corresponding energy would give a flip rate of 0.2 cps in channel A and 0.3 cps in channel B. A glance at the graph shows that these are close to the observed rates. The fact that detector A contains the broom magnet may explain the lower response of this detector.

---

22. Artificial Earth Satellites, L. V. Kurnosova, Editor: Soviet Ionospheric Studies Using Rockets and Artificial Earth Satellites, V. I. Krasovskii, page 45, Plenum Press, Inc., 1960.

V. CONCLUSION

In view of the performance of the CdS total energy detector in the laboratory and the brief flight data, it is the opinion of the author that on the occasion of its use, the detector discussed will make a significant contribution to the understanding of the earth's corpuscular radiation environment.

REFERENCES

1. J. A. Van Allen, "The Geomagnetically-Trapped Corpuscular Radiation", J. Geophys. Research 64, 1683-1689 (1959).

2. Albert Rose, "Performance of Photoconductors", in R. G. Breckenridge, B. R. Russell, E. E. Hahn (editors), "Photoconductivity Conference", Section IA, pp. 3-48, John Wiley and Sons, Inc., New York, 1956, page 3.

3. R. H. Bube, "Photoconductivity of Solids", John Wiley and Sons, Inc., New York, 1960, page 31.

4. See reference 2 above, page 5.

5. See reference 2 above, page 9.

6. Charles Kittel, "Introduction to Solid State Physics", John Wiley and Sons, Inc., New York, 1956, page 526.

7. See reference 6 above, page 59.

8. E. Fermi (Orear, Rosenfeld, Scheuter), "Nuclear Physics", University of Chicago Press.

9. See reference 6 above, page 529.

10. American Institute of Physics Handbook, McGraw-Hill, New York, 1957, pp. 8-251.

11. A. H. Compton and S. K. Allison, X-Rays in Theory and Experiment, D. Van Nostrand Co., 1955, Appendix IX.

12. R. T. McGinnies, X-Ray Attenuation Coefficients from 10 kev to 100 Mev, National Bureau of Standards Circular 583 Supplement.

13. See reference 3 above, page 269.

14. See reference 3 above, page 59; and reference 2 above, page 11.

15. "Handbook of Physics", E. U. Condon and H. Odishaw, editors: Chapter 8, X-Rays, E. U. Condon, McGraw-Hill Book Company, New York, 1958.

16. S. N. Vernov, Special Lecture, Fifth General Assembly of C.S.A.G.I., Moscow, July 30-August 9, 1958.

17. G. H. Ludwig, "The Development of a Corpuscular Radiation Experiment for an Earth Satellite", Ph.D. dissertation, State University of Iowa (August 1960).

18. Sears and Zemansky, University Physics, Addison Wesley Publishing Co., 1953.

19. Orear, Jay, "Fundamental Physics", John Wiley and Sons, Inc., 1960, page 331.

20. C. W. Allen, "Astrophysical Quantities", The Athlone Press, page 231.

21. M. J. Seaton, Journal of Atmospheric and Terrestrial Physics, Vol. 4 (1954), pp. 285-294.

22. Artificial Earth Satellites, L. V. Kurnosova, Editor: Soviet Ionospheric Studies Using Rockets and Artificial Earth Satellites, V. I. Krasovskii, page 45, Plenum Press, Inc., 1960.

CAPTIONS FOR FIGURES

Fig. 1 A schematic energy level diagram for a typical photoconductor showing the relative positions of the valence and conduction bands and the shallow and deep traps in the forbidden zone.

Fig. 2 The electron gun and beam monitoring setup for measuring the electron sensitivity of CdS crystals.

Fig. 3 Graph showing the independence of crystal electron sensitivity to electron beam energy flux.

Fig. 4 Graph showing the independence of crystal electron sensitivity to electron energy.

Fig. 5 Graph showing the dependence of crystal proton sensitivity to proton energy.

Fig. 6 Graph showing the similarity of crystal electron sensitivity to crystal proton sensitivity.

Fig. 7 Graph showing the linearity of crystal response to a 230 KV X-ray beam.

Fig. 8 Graph showing the response of CdS crystals to a constant intensity beta source as a function of temperature.

Fig. 9 Schematic diagram for circuits used to measure the response time of CdS crystals.

Fig. 10 Oscilloscope traces of the rise and fall times of the photocurrent in a CdS crystal following a step function in the incident radiation.

Fig. 11 The response time (rise) as a function of final photocurrent and temperature.

Fig. 12 Detector response following the removal of low level incident radiation.

CAPTIONS FOR FIGURES
(continued)

Fig. 13 A cross sectional drawing of the complete CdS detector without magnet.

Fig. 14 Graph showing the response of the detector to a 500 watt projector at various angles with the detector axis.

Fig. 15 A cross sectional drawing of the complete CdS detector with magnet.

Fig. 16 Schematic diagram of the crystal circuit and pulse forming circuit.

Fig. 17 A typical calibration curve for the current to frequency converter circuit.

Fig. 18 A typical calibration curve for the CdS detector including the current to frequency converter.

Fig. 19 Schematic diagram showing the 160 volt power supply for the CdS detector.

Fig. 20 S-46 Launch Data showing the response of the 2 CdS detectors to various light sources during the tilt program and the high speed stage ignitions.

Fig. 21 The assembled CdS detector.

Fig. 22 An exploded view of the entire detector showing the light baffles, the magnet, the crystal and current to frequency converter.

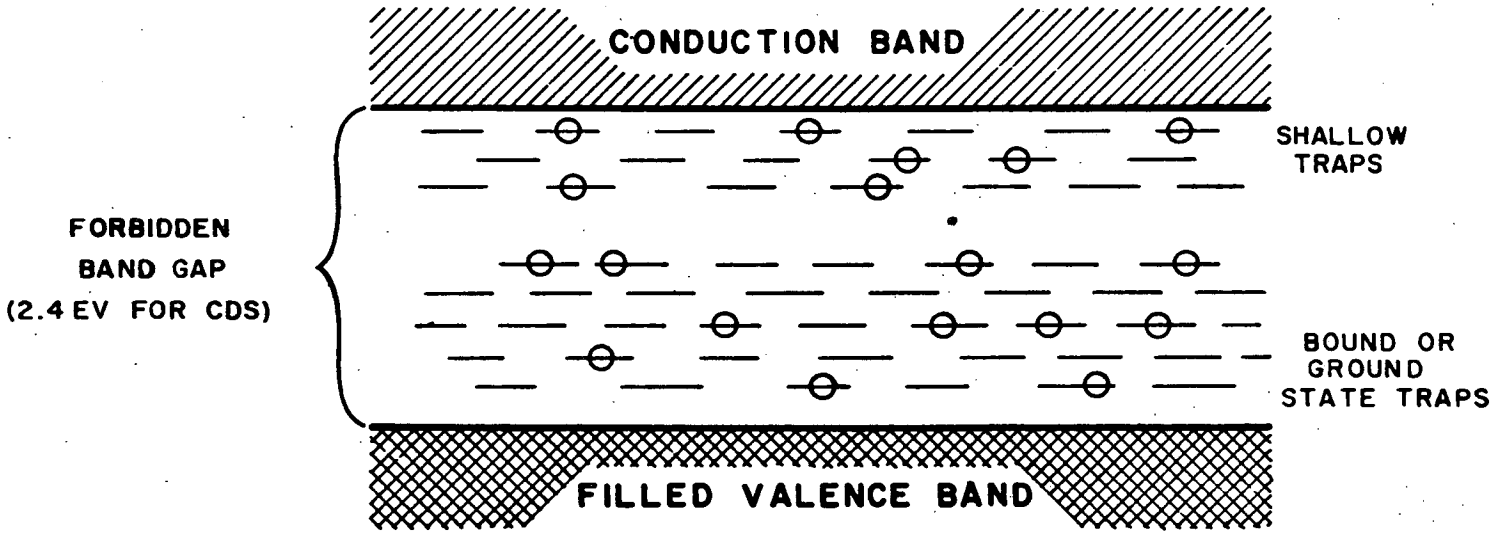

FIG.1 SCHEMATIC ENERGY LEVEL DIAGRAM FOR TYPICAL PHOTOCONDUCTOR

Fig. 1

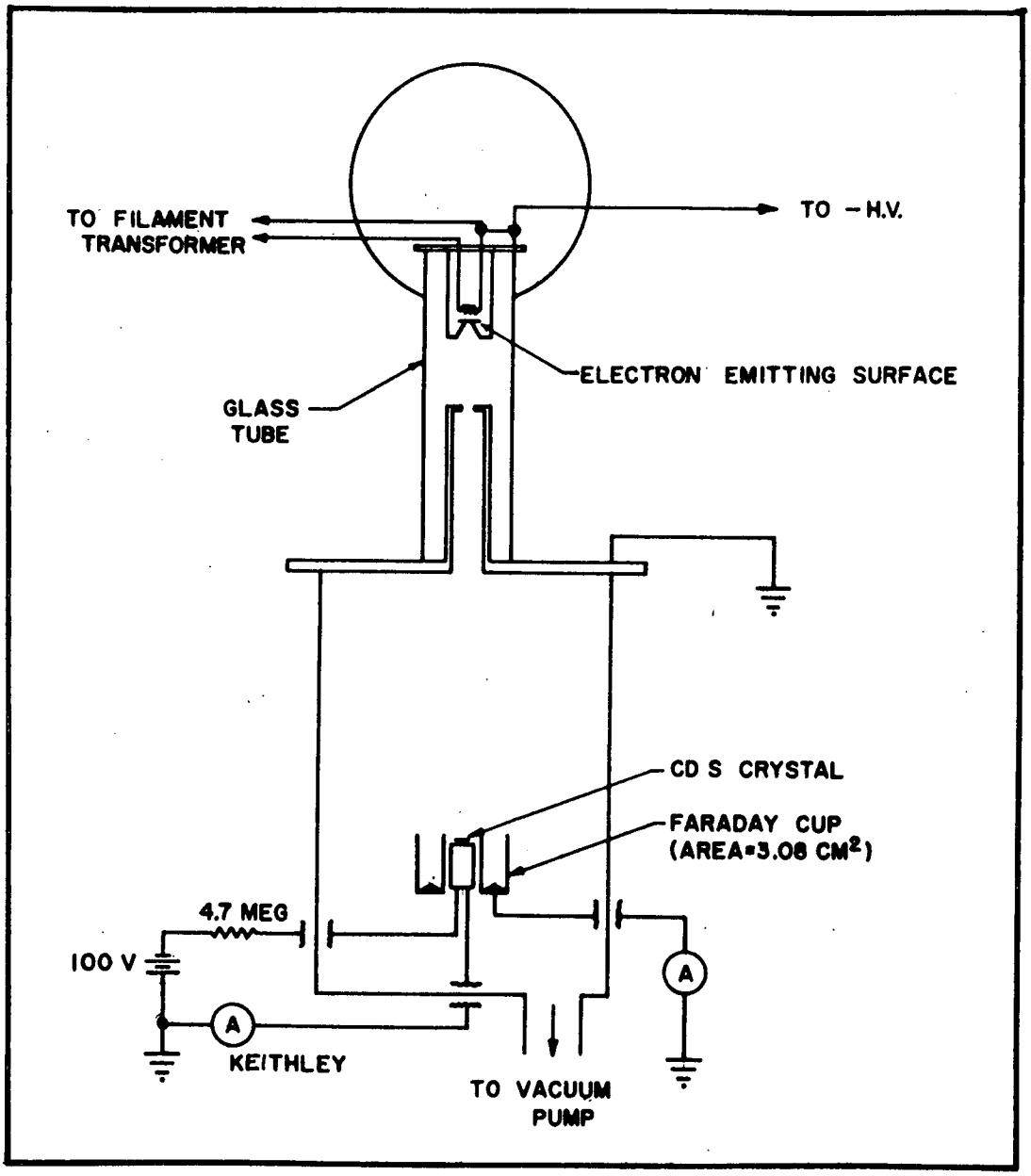

FIG. 2 APPARATUS FOR MEASURING ELECTRON SENSITIVITY OF CD.S. CRYSTALS

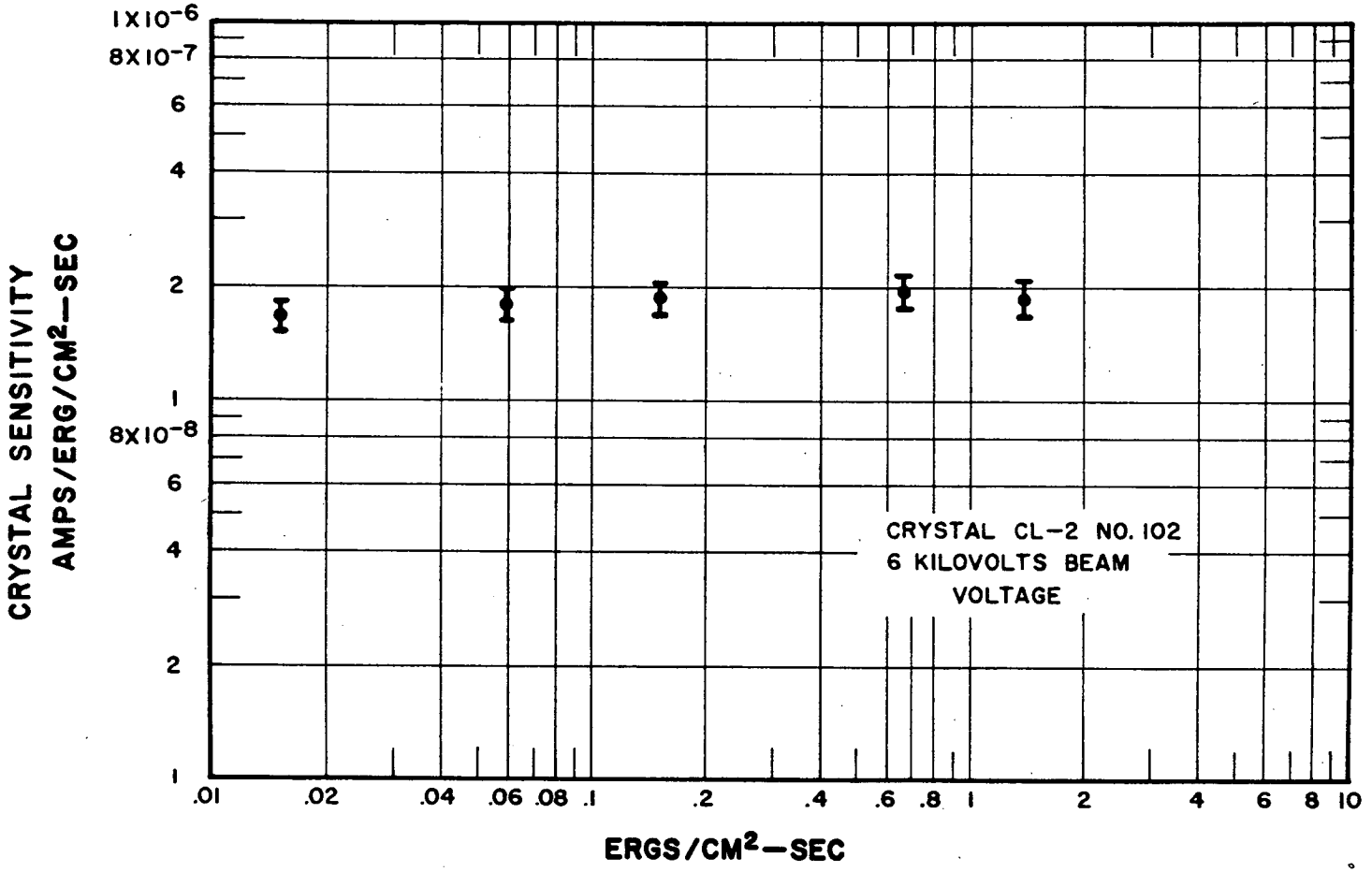

FIG.3 CRYSTAL SENSITIVITY VS. BEAM ENERGY FLUX FOR CONSTANT ELECTRON ENERGY

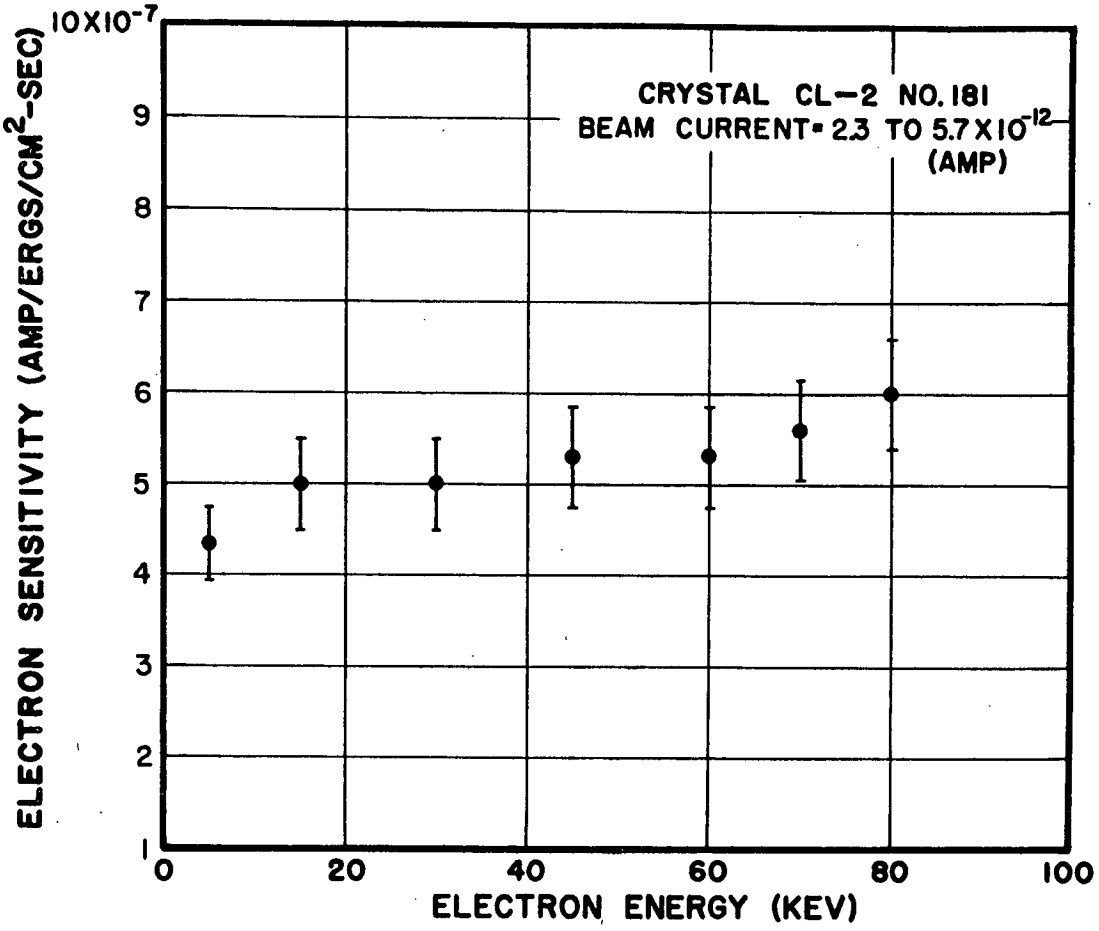

FIG. 4 ELECTRON SENSITIVITY VS. ELECTRON ENERGY FOR CONSTANT BEAM CURRENT

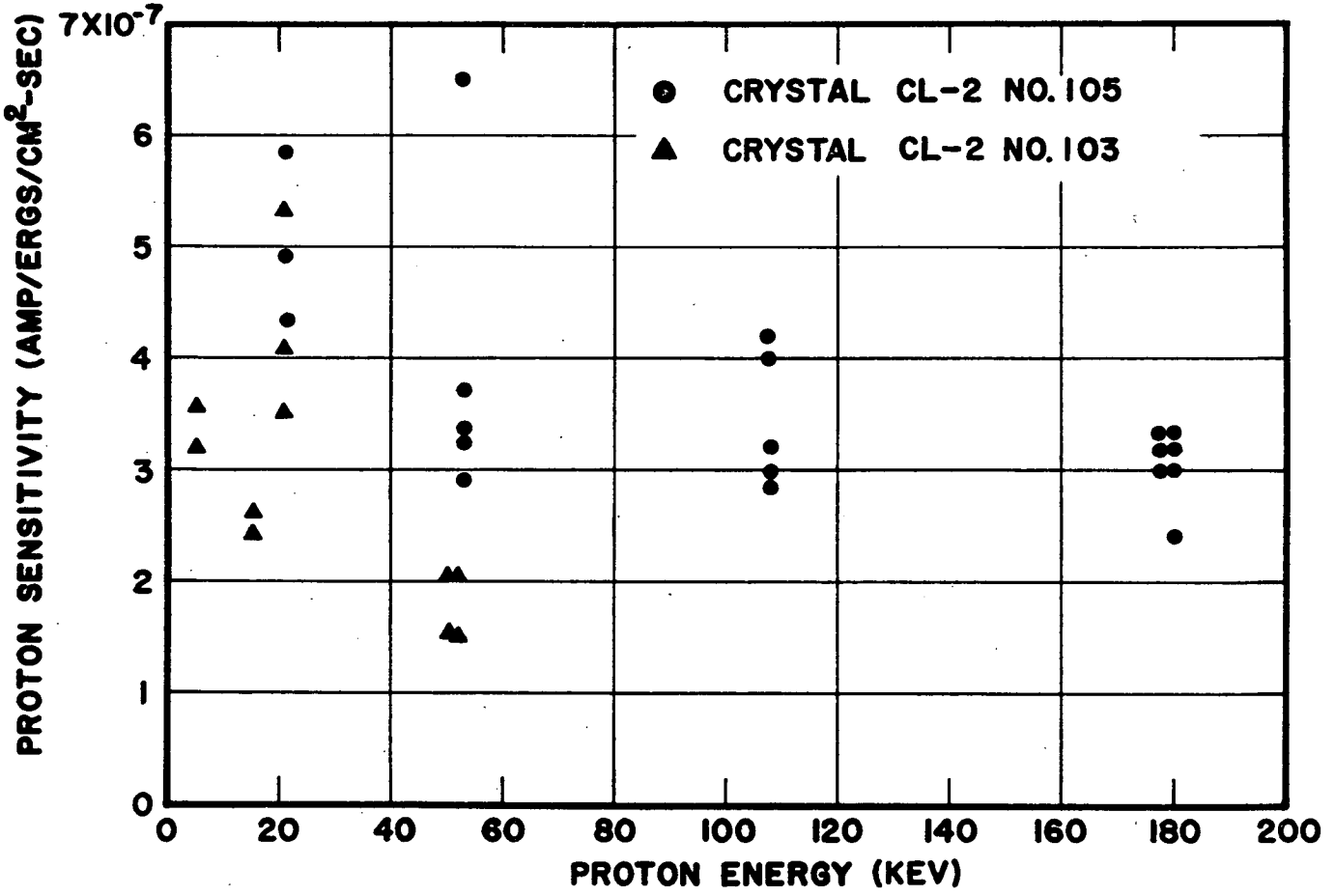

FIG. 5:
PROTON SENSITIVITY VS. PROTON ENERGY

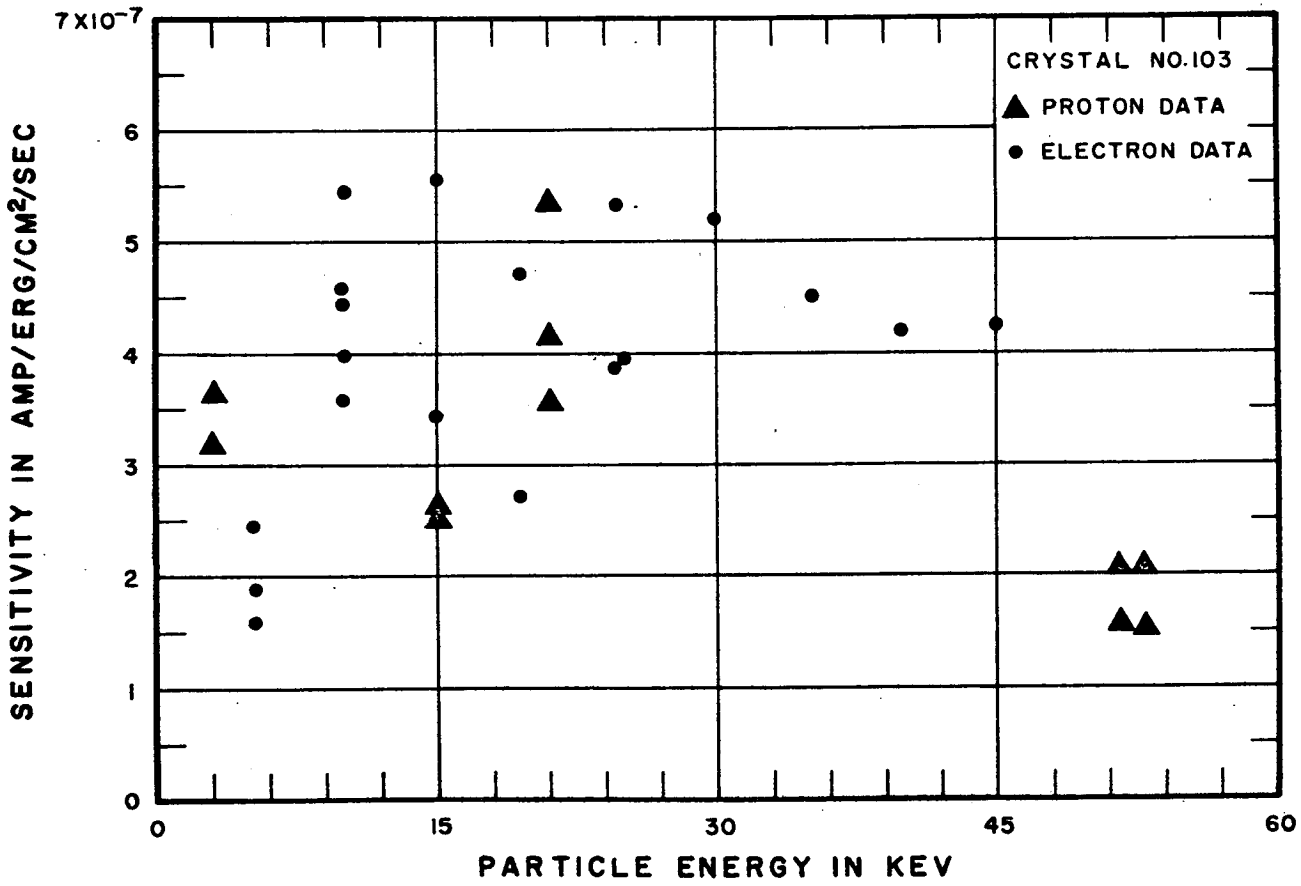

FIG. 6 PROTON AND ELECTRON SENSITIVITY
VS.
PARTICLE ENERGY

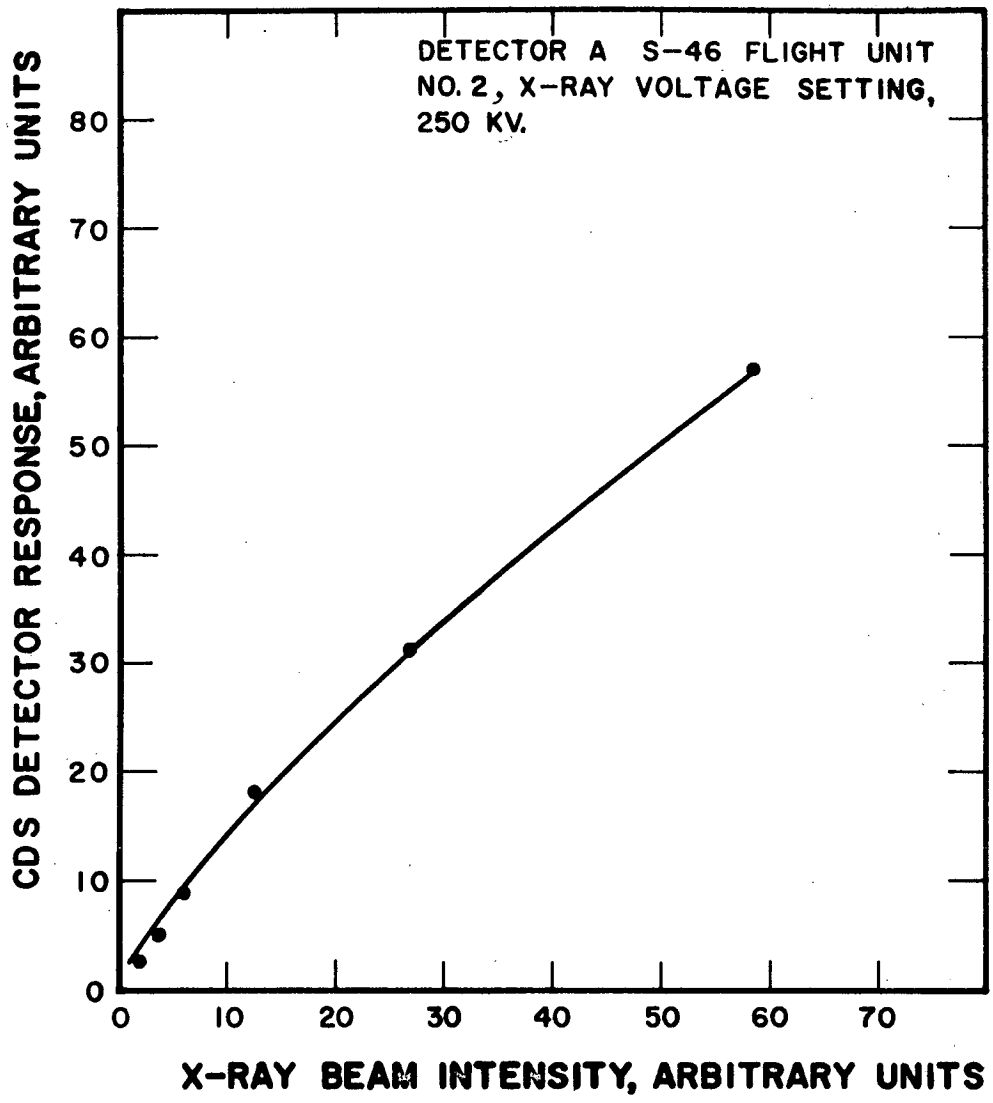

FIG. 7 X-RAY BEAM INTENSITY VS. CD S DETECTOR RESPONSE FOR AN INVERSE SQUARE LAW TEST

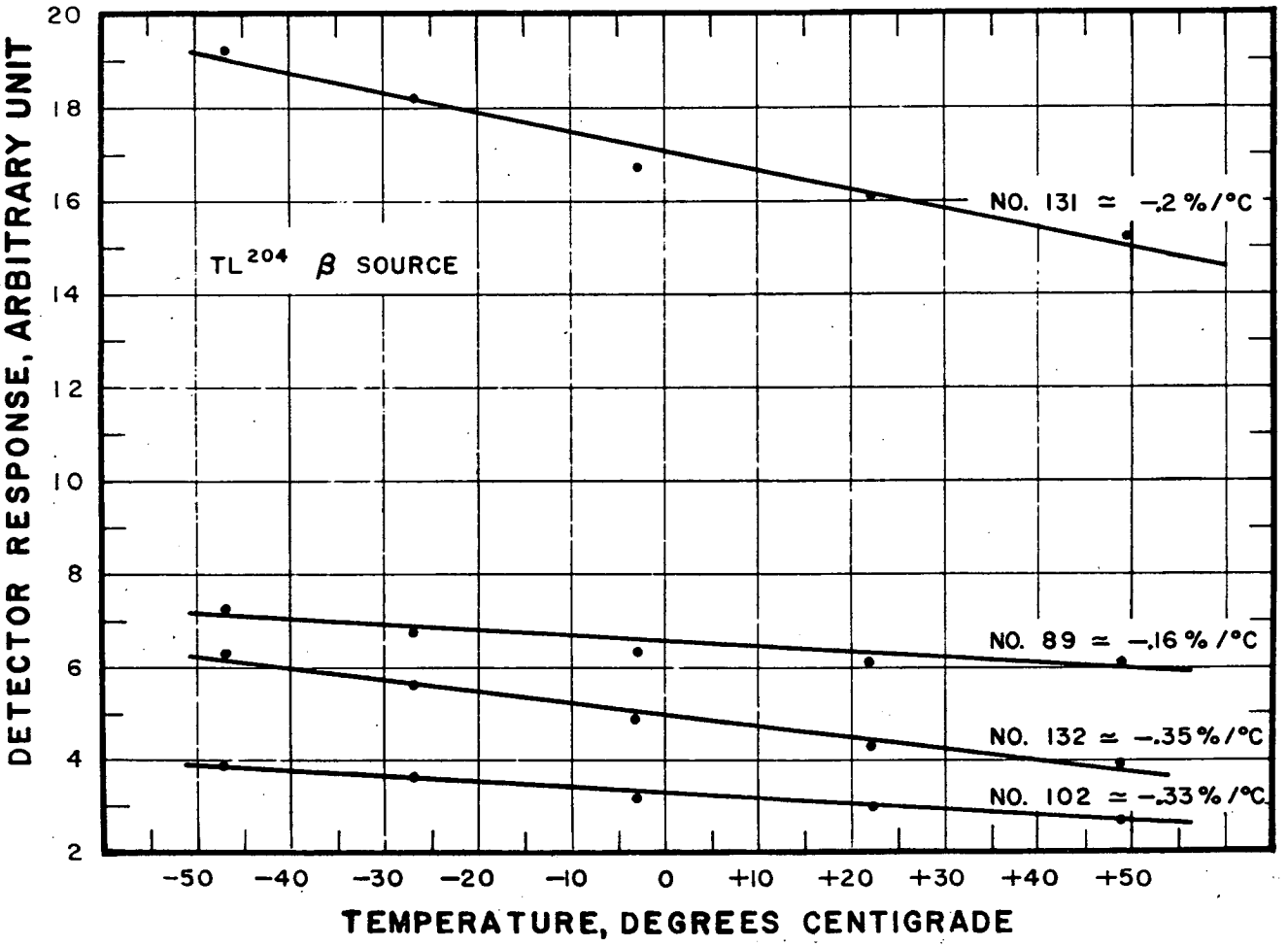

FIG. 8 CDS CRYSTAL RESPONSE VS TEMPERATURE

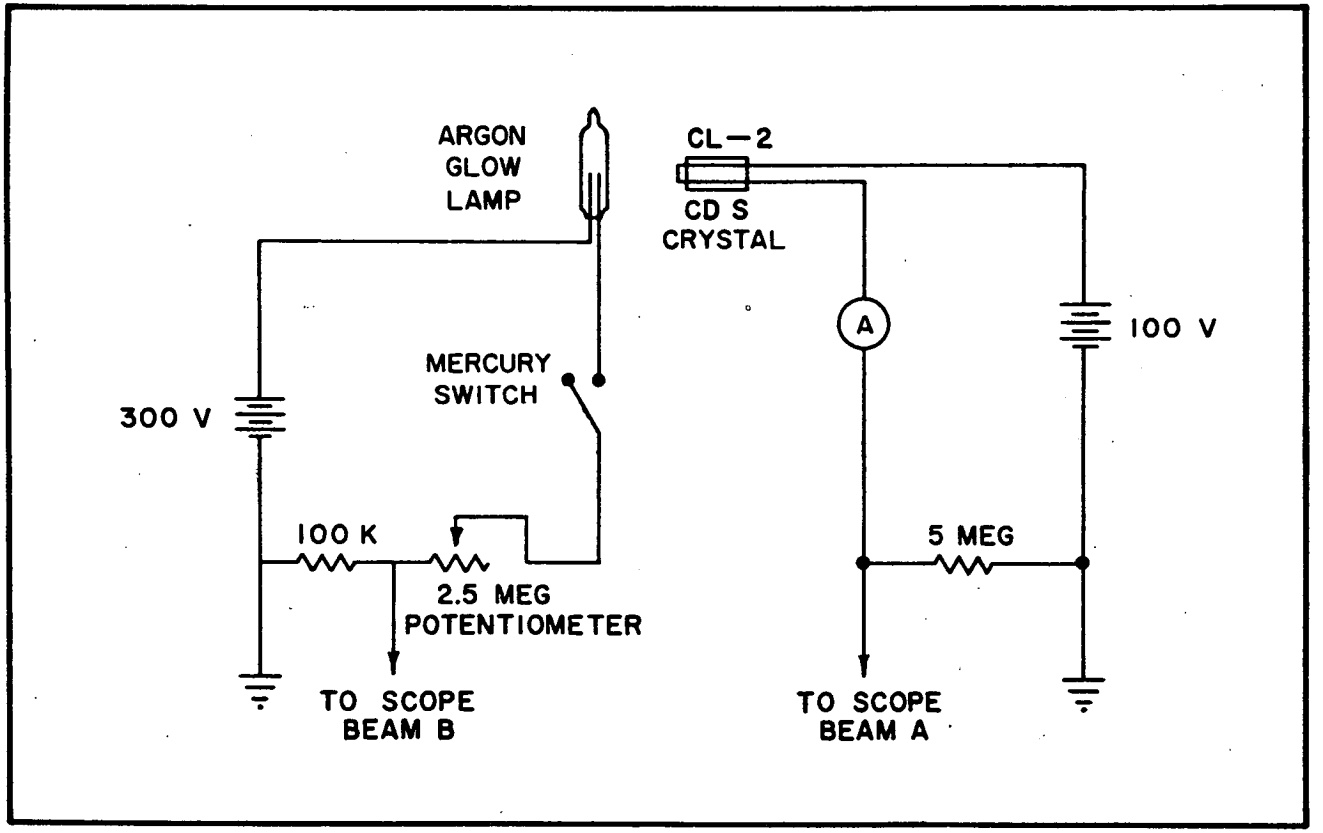

FIG. 9
RESPONSE TIME MEASURING SETUP FOR HIGH CURRENTS

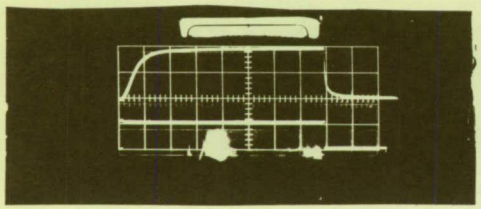

I_C (FINAL) = 10^{-5} AMP
100 MSEC/CM
RISE TIME ≅ 150 MSEC
FALL TIME ≅ 25 MSEC

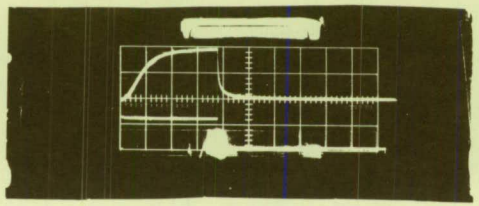

I_C (FINAL) = 5×10^{-6} AMP
100 MSEC/CM
RISE TIME ≅ 200 MSEC
FALL TIME ≅ 50 MSEC

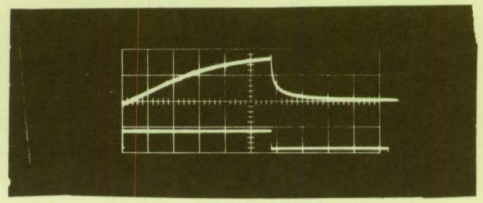

I_C (FINAL) = 10^{-6} AMP
100 MSEC/CM
RISE TIME ≅ 600 MSEC
FALL TIME ≅ 100 MSEC

UPPER BEAM: PHOTOCURRENT
LOWER BEAM: ARGON LAMP CURRENT

THE LIGHT SWITCH IS CONTROLLED MANUALLY

FIG. 10 RESPONSE TIME CURVES FOR HIGH CRYSTAL CURRENT

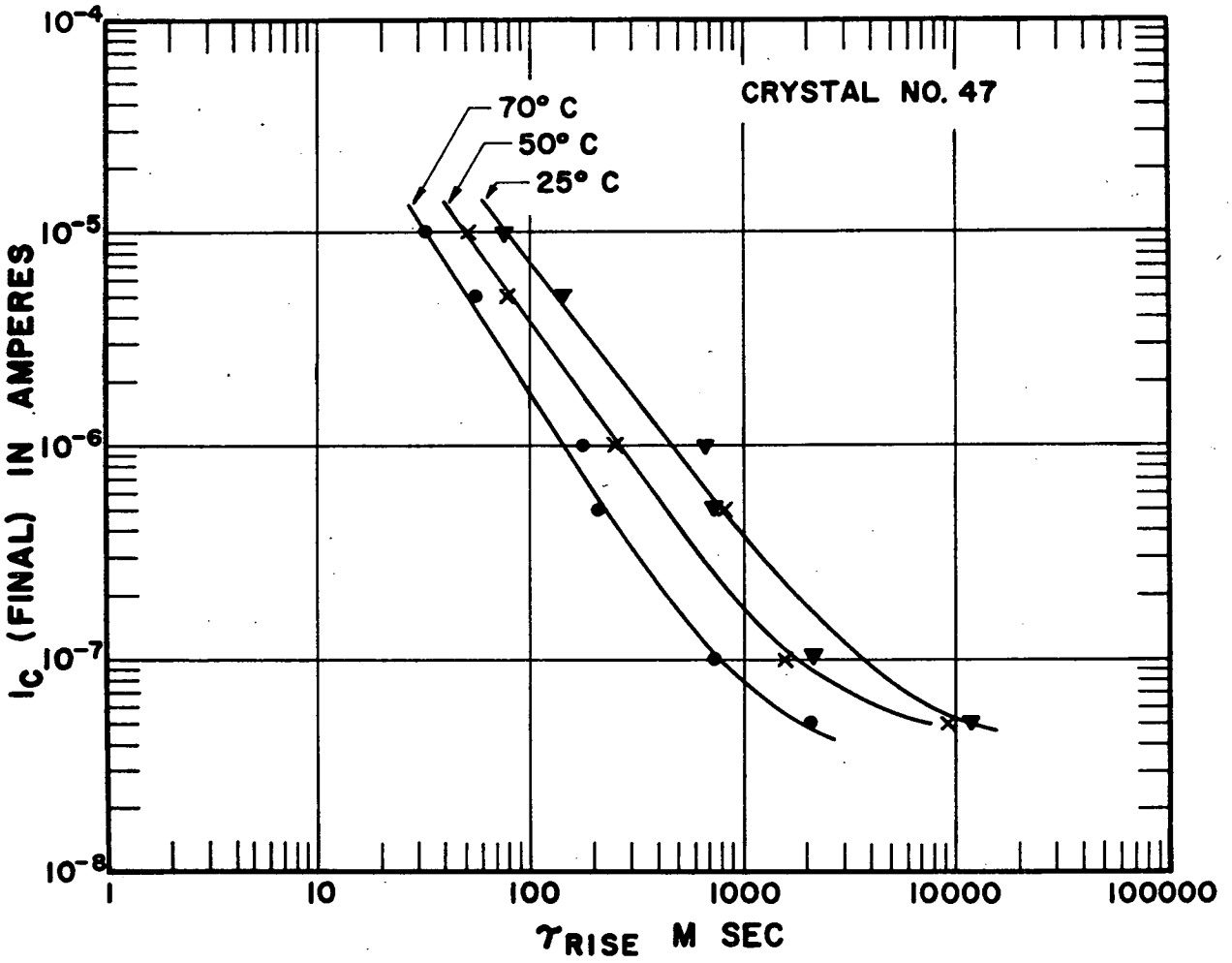

FIG. 11
RESPONSE TIME (RISE) VS. FINAL CRYSTAL CURRENT WITH TEMPERATURE AS A 3rd. PARAMETER

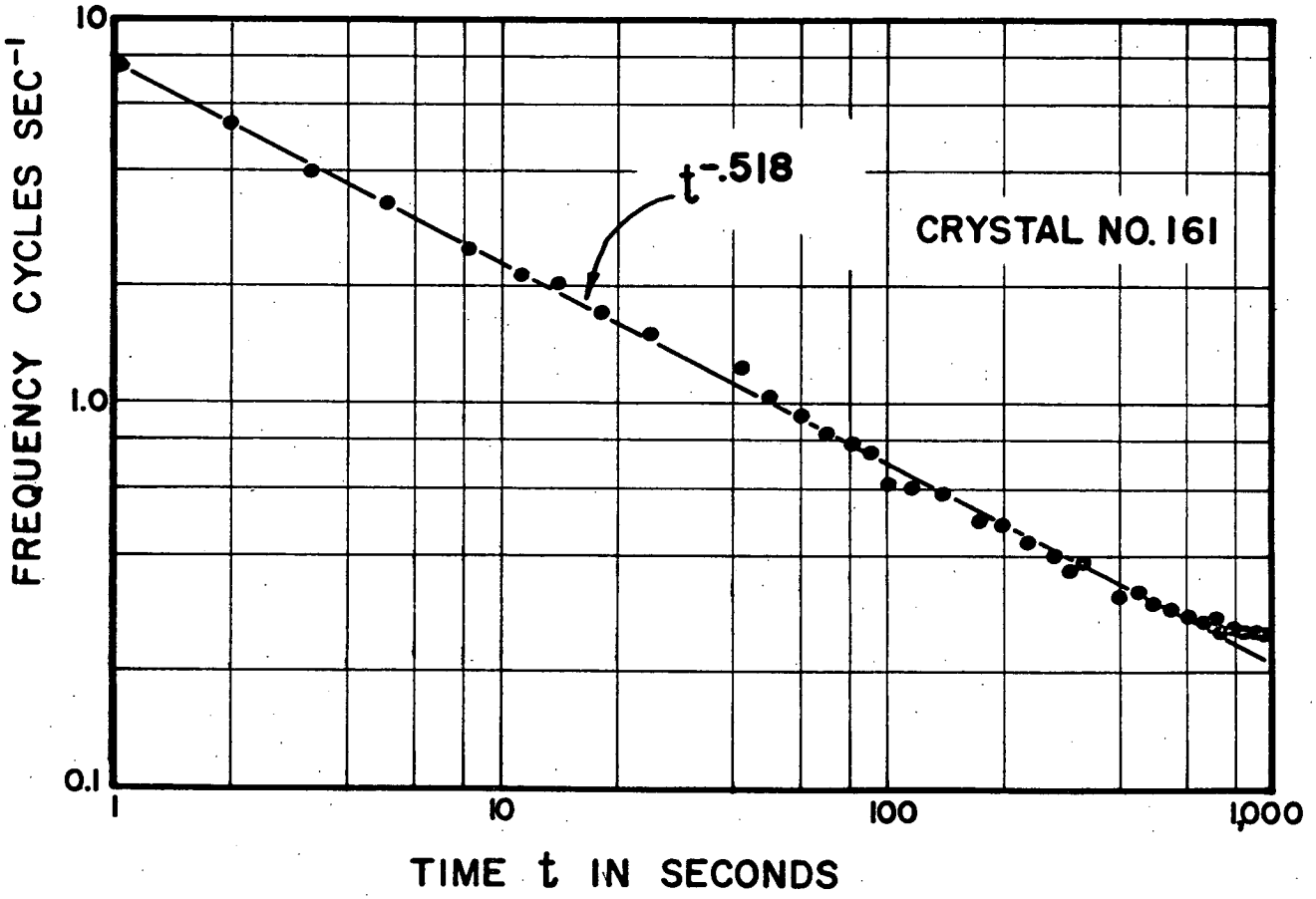

FIG. 12 DETECTOR RESPONSE VS TIME FOR LIGHT OFF AT t=1 SECOND

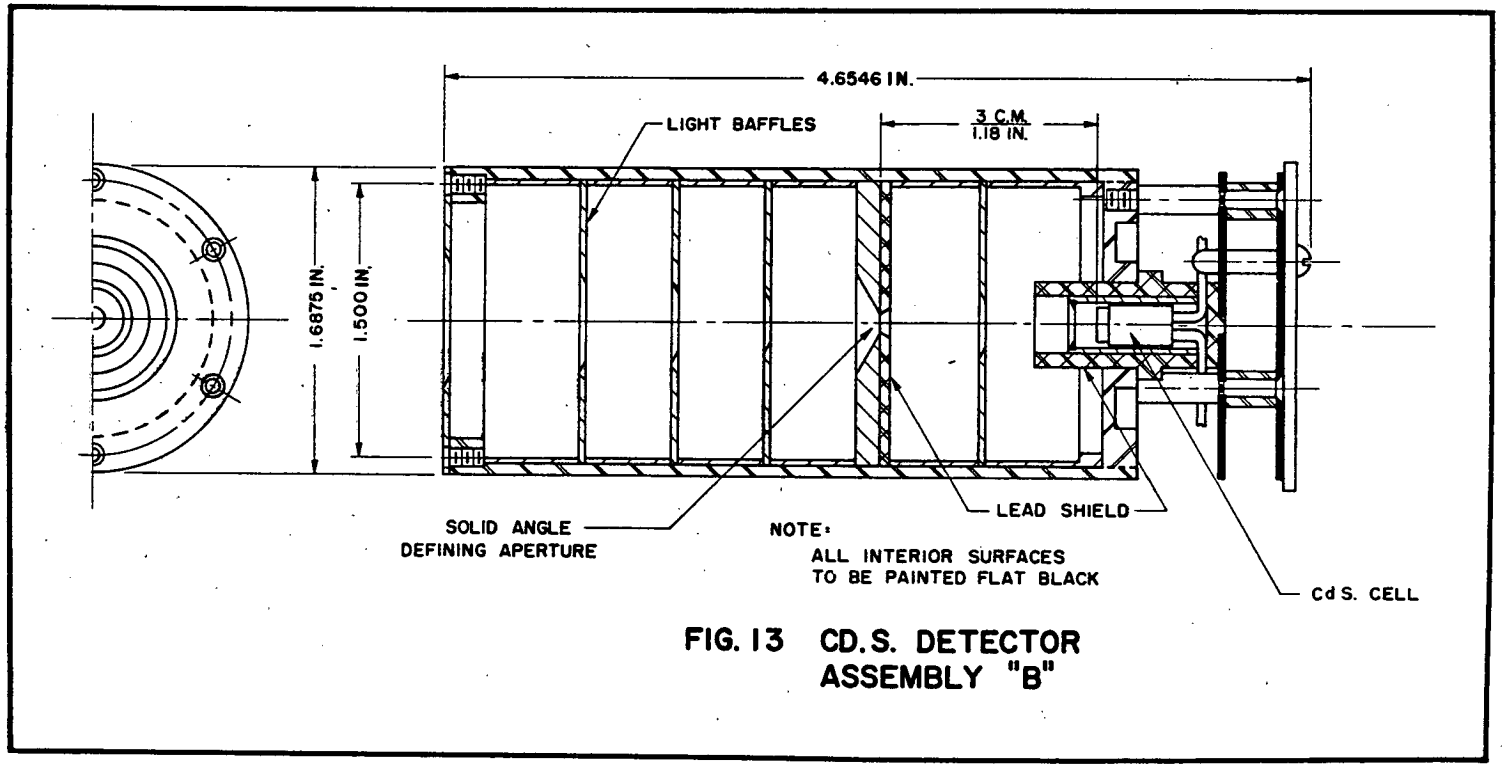

FIG. 13 CD.S. DETECTOR ASSEMBLY "B"

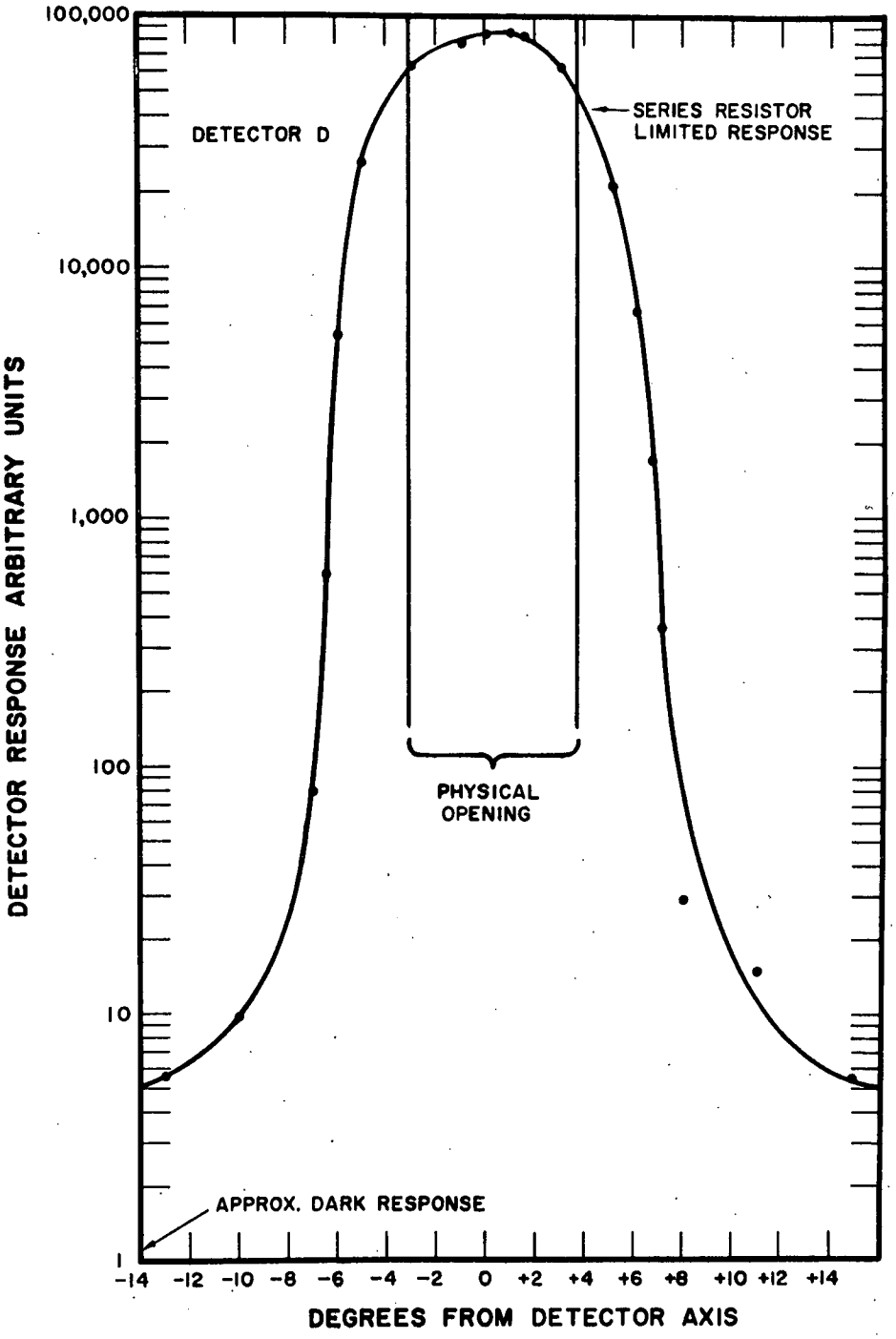

FIG. 14 LIGHT BAFFLE EFFICIENCY
FOR 500 WATT PROJECTOR

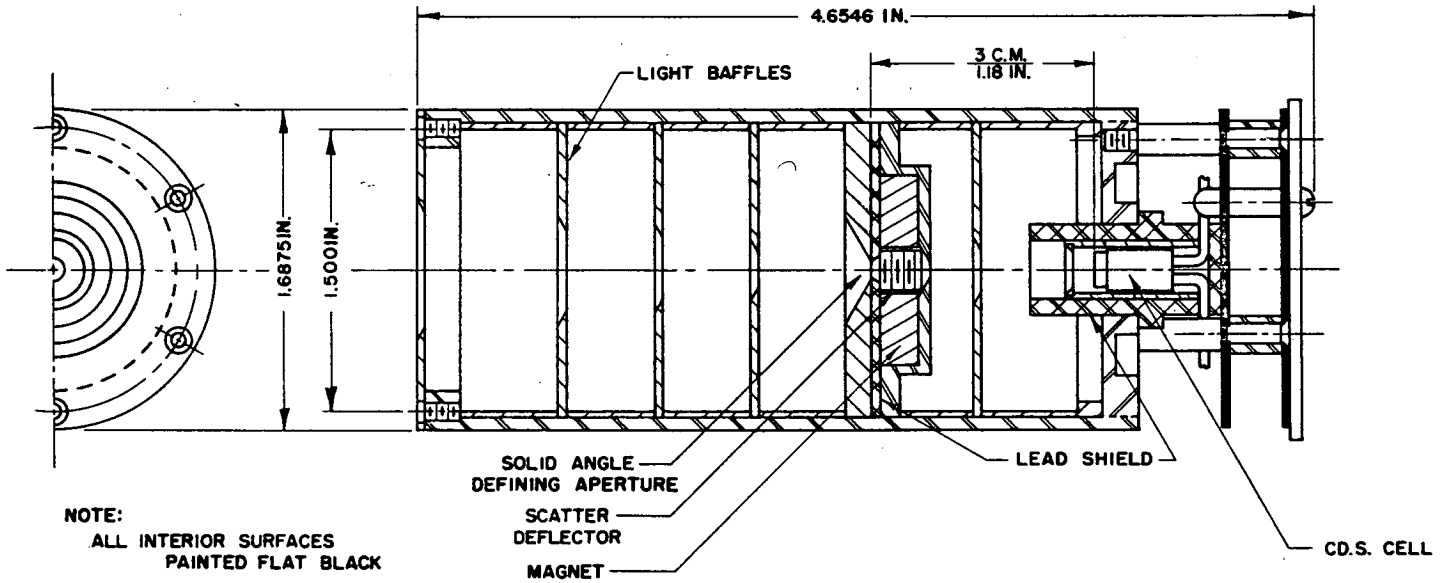

FIG. 15 CD.S. DETECTOR ASSEMBLY "A"

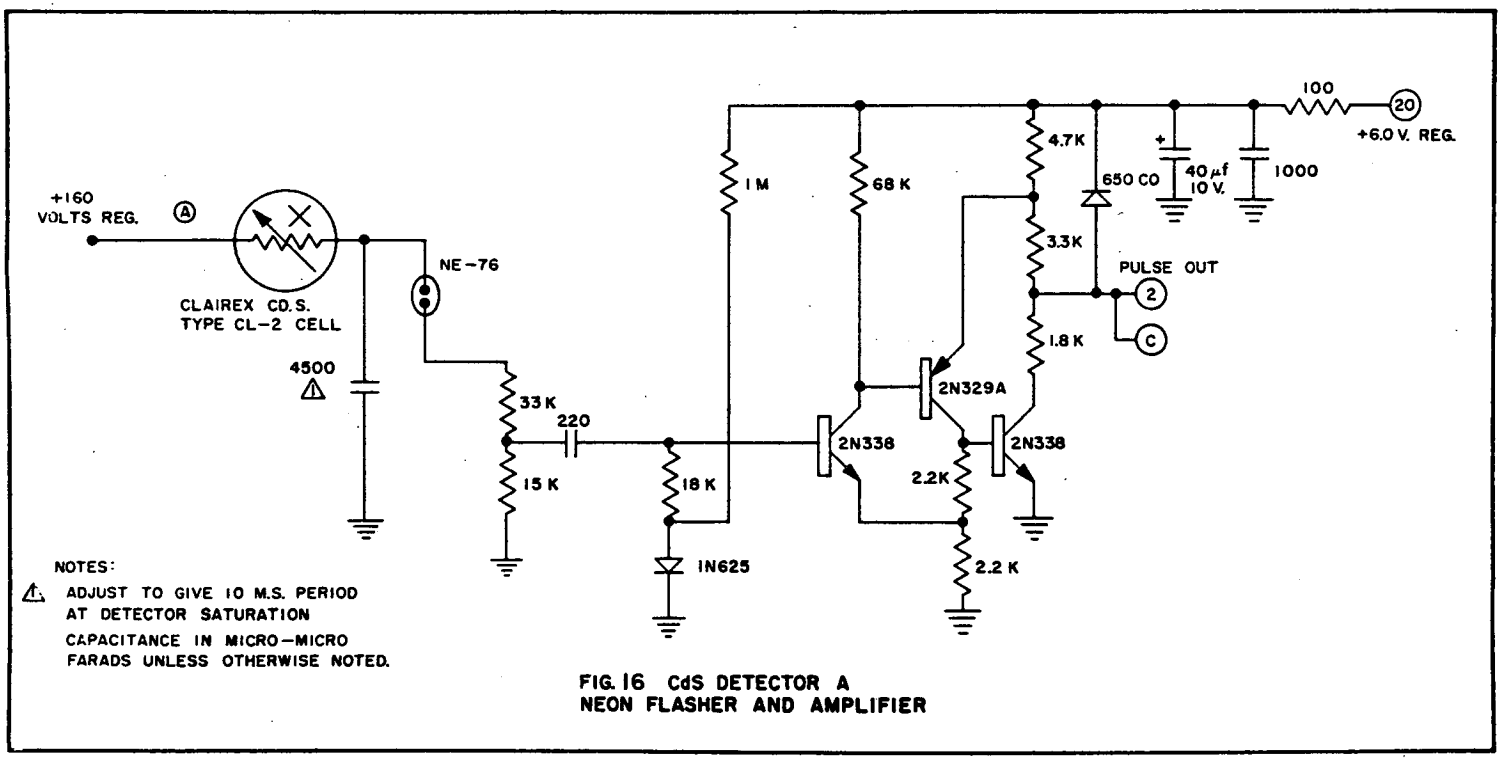

FIG. 16 CdS DETECTOR A
NEON FLASHER AND AMPLIFIER

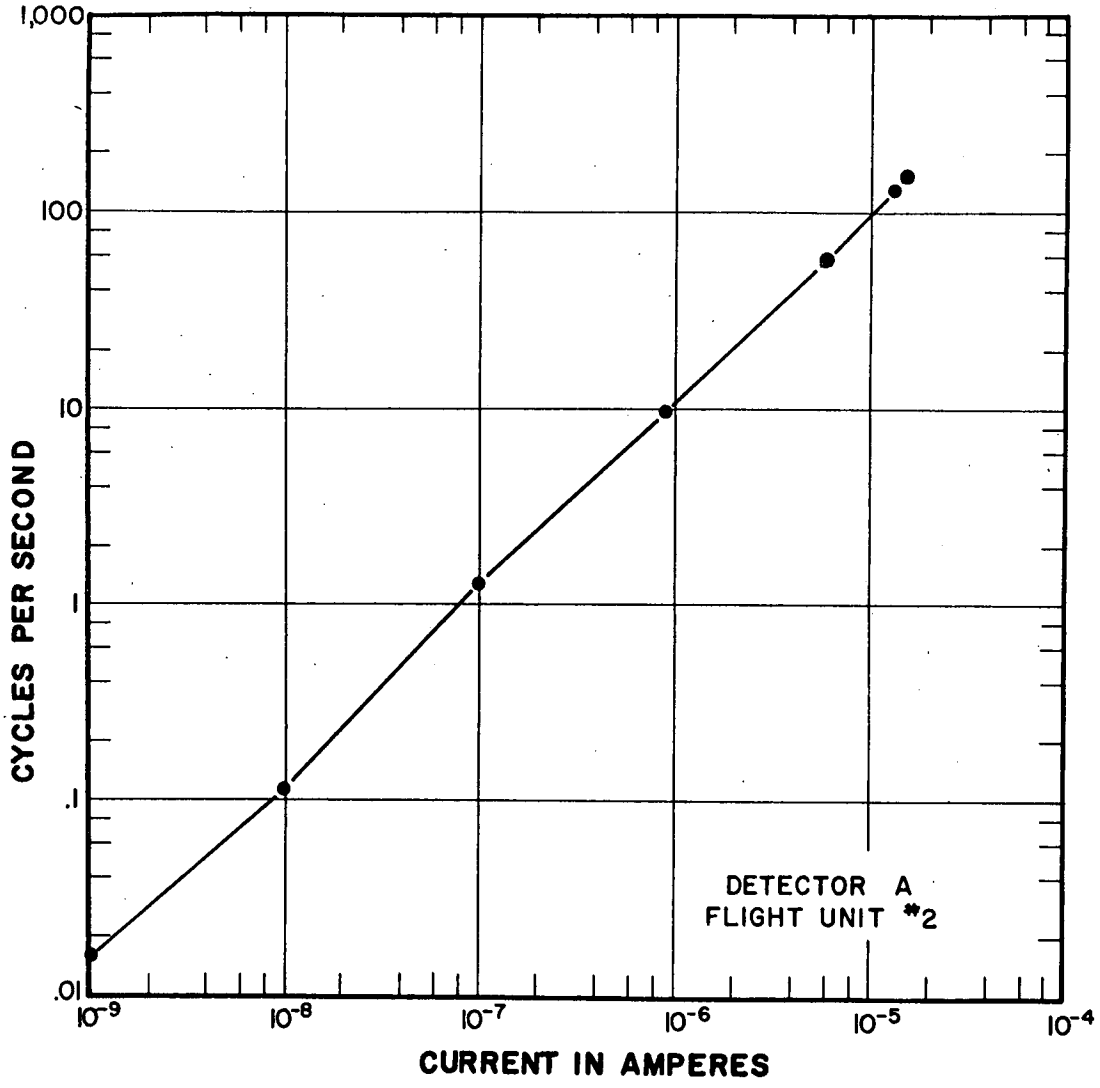

FIG. 17 ANALOG TO FREQUENCY CONVERTER CALIBRATION CURVE

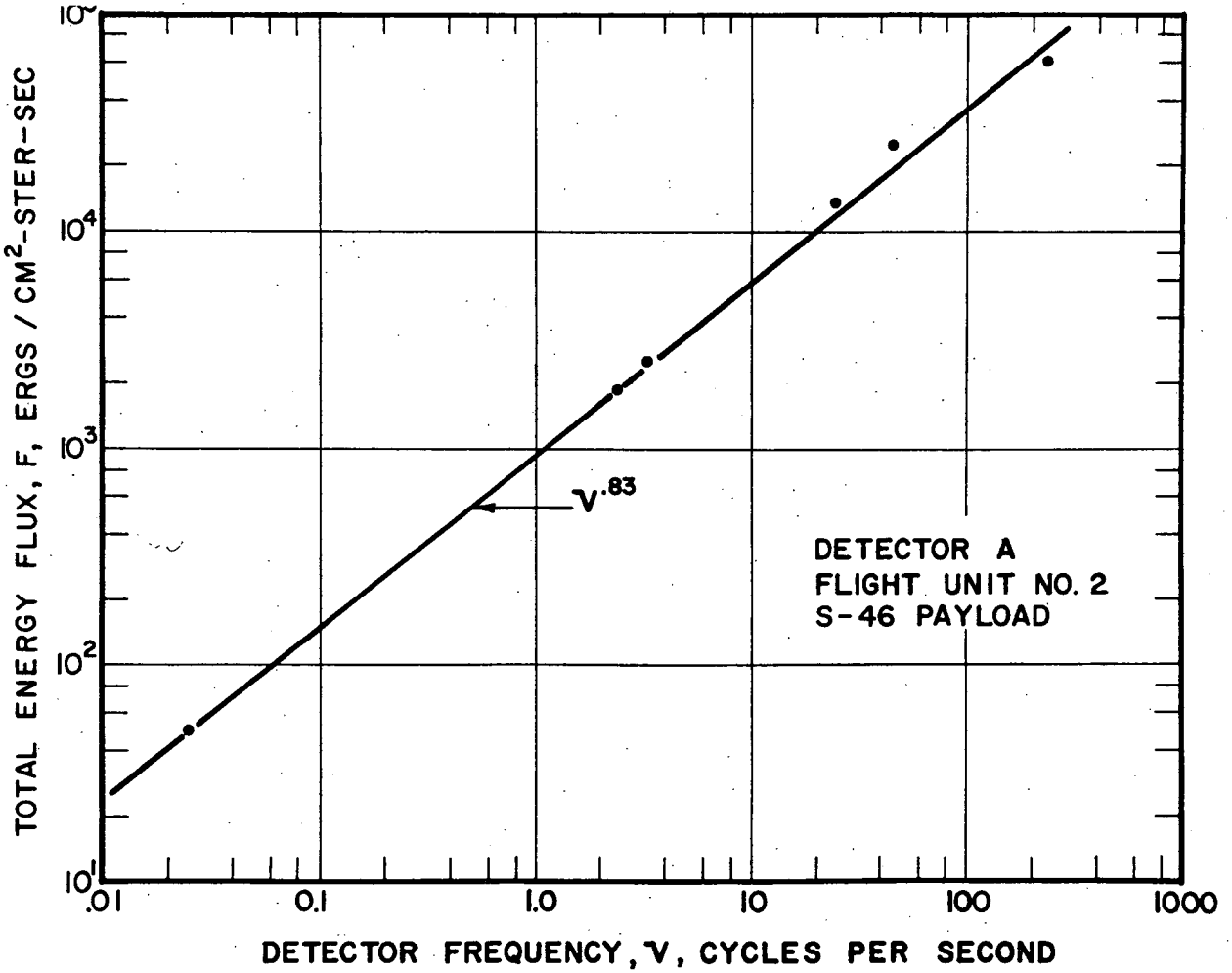

FIG. 18 TOTAL ENERGY FLUX VS DETECTOR FREQUENCY

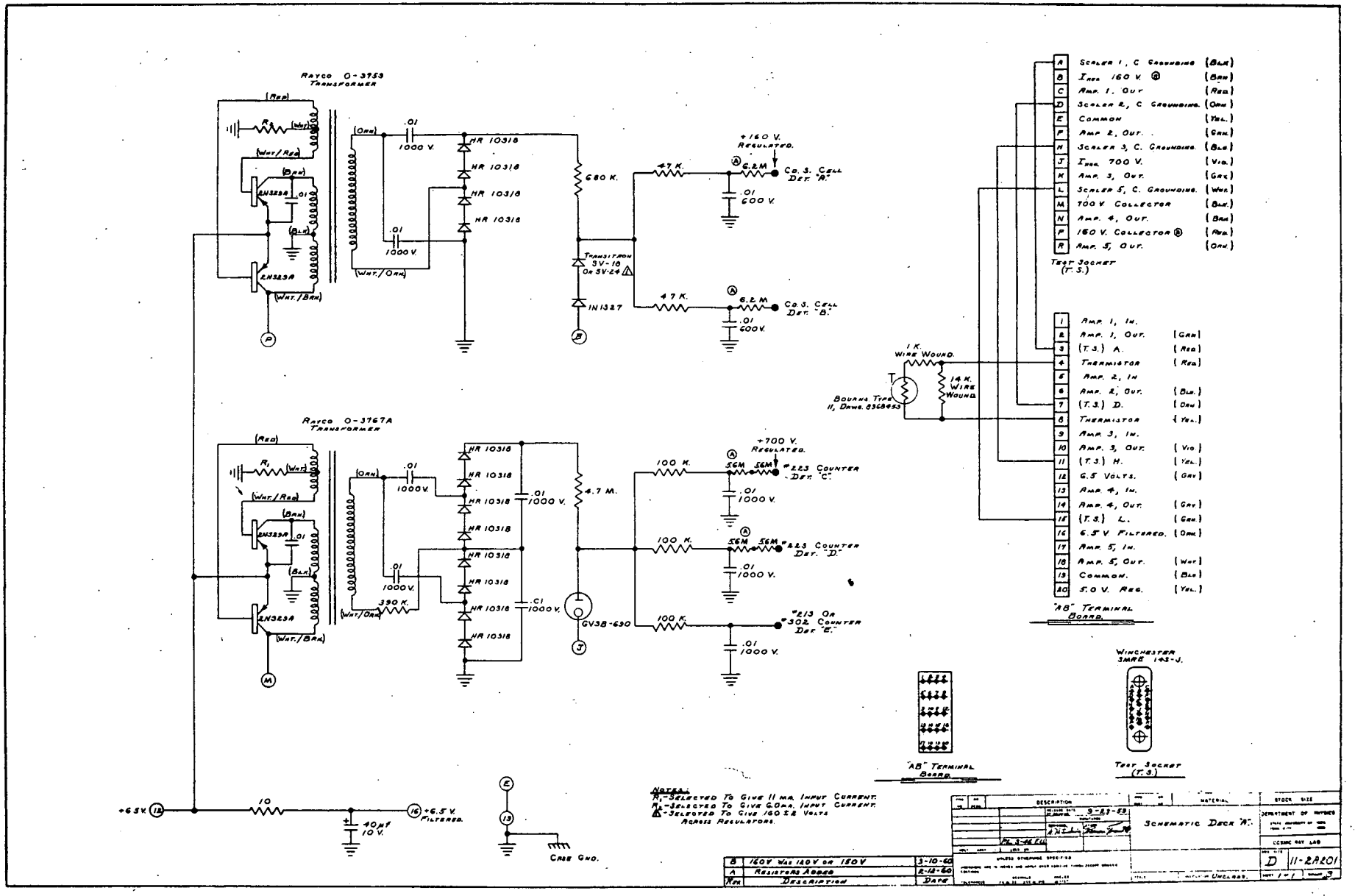
Rayco 0-3759 Transformer
Rayco 0-3767A Transformer
+160 V. Regulated.
+700 V. Regulated.
Transition 3V-16 or 3V-24
IN1327
GV38-690
Co. 3. Cell Det. "A."
Co. 3. Cell Det. "B."
"223 Counter Det. "C."
"223 Counter Det. "D."
"213 Or "302 Counter Det. "E."
Bourns Type 11, Drwg. 6368953
1 K. Wire Wound.
14 K. Wire Wound.
Test Socket (T.S.)
"AB" Terminal Board.
Winchester 3MPE 143-J.
+6.5 V.
+6.5 V. Filtered.
Case Gnd.
Notes:
R1-Selected To Give 11 ma. Input Current.
R2-Selected To Give 6.0 ma. Input Current.
Δ-Selected To Give 160 ± 2 Volts Across Regulator.
Schematic Deck "A"
Uncl.
D 11-2A201

Fig. 19

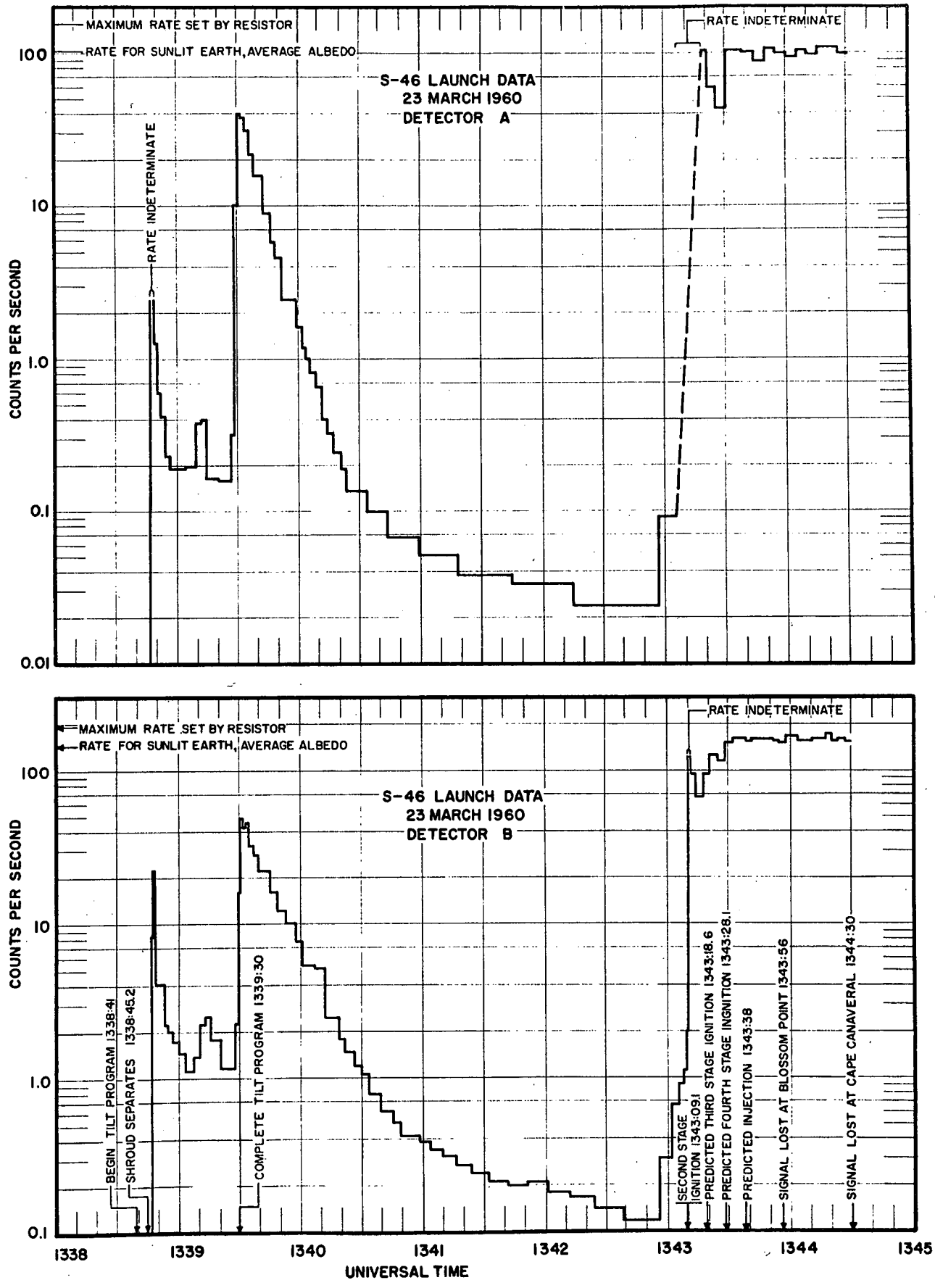
MAXIMUM RATE SET BY RESISTOR
RATE FOR SUNLIT EARTH, AVERAGE ALBEDO
RATE INDETERMINATE
S-46 LAUNCH DATA
23 MARCH 1960
DETECTOR A
RATE INDETERMINATE
COUNTS PER SECOND
100
10
1.0
0.1
0.01
MAXIMUM RATE SET BY RESISTOR
RATE FOR SUNLIT EARTH, AVERAGE ALBEDO
RATE INDETERMINATE
S-46 LAUNCH DATA
23 MARCH 1960
DETECTOR B
COUNTS PER SECOND
100
10
1.0
0.1
BEGIN TILT PROGRAM 1338:41
SHROUD SEPARATES 1338:45.2
COMPLETE TILT PROGRAM 1339:30
SECOND STAGE IGNITION 1343:09.1
PREDICTED THIRD STAGE IGNITION 1343:18.6
PREDICTED FOURTH STAGE INGNITION 1343:28.1
PREDICTED INJECTION 1343:38
SIGNAL LOST AT BLOSSOM POINT 1343:56
SIGNAL LOST AT CAPE CANAVERAL 1344:30
1338
1339
1340
1341
1342
1343
1344
1345
UNIVERSAL TIME

Fig. 20

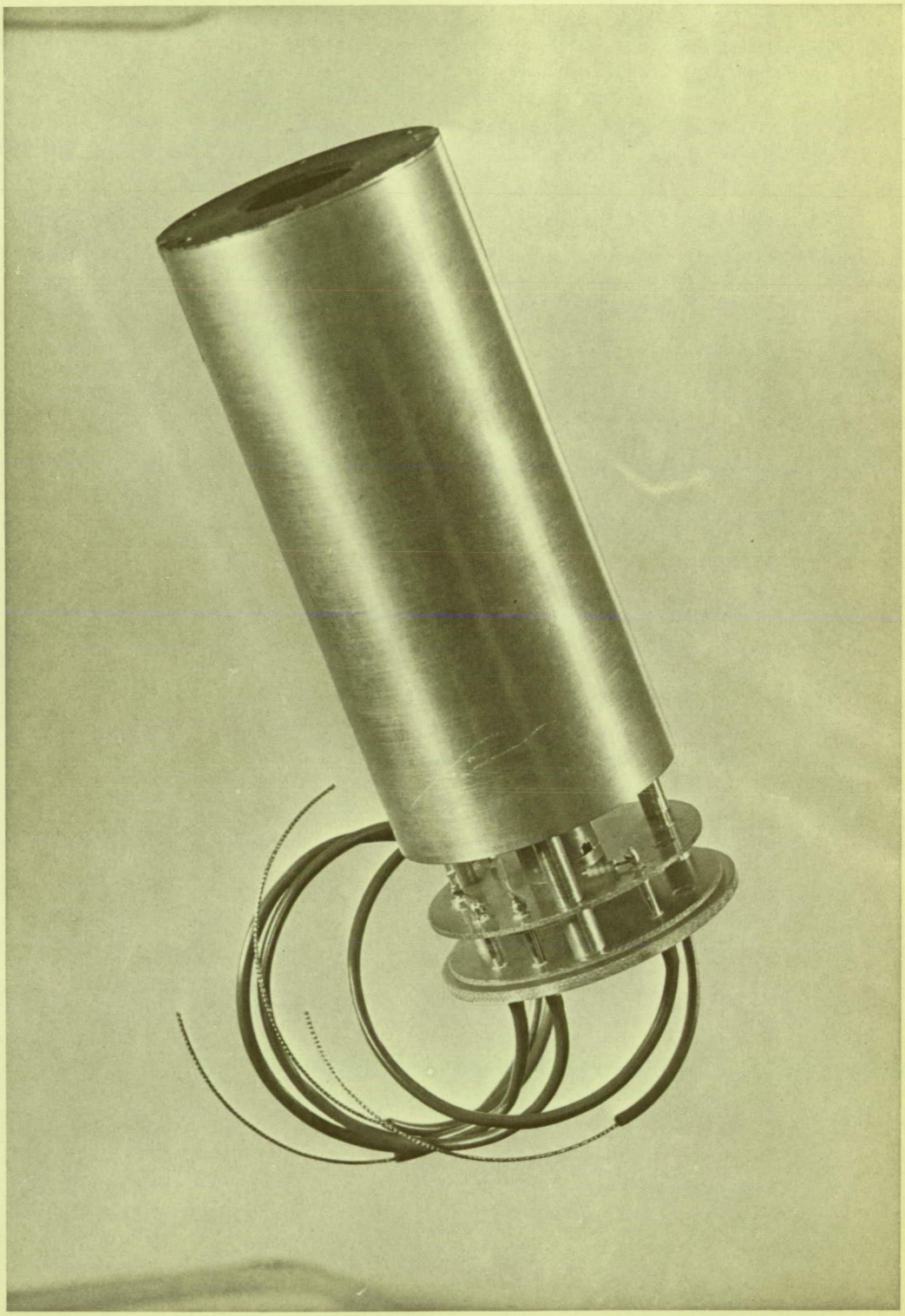

Fig. 21

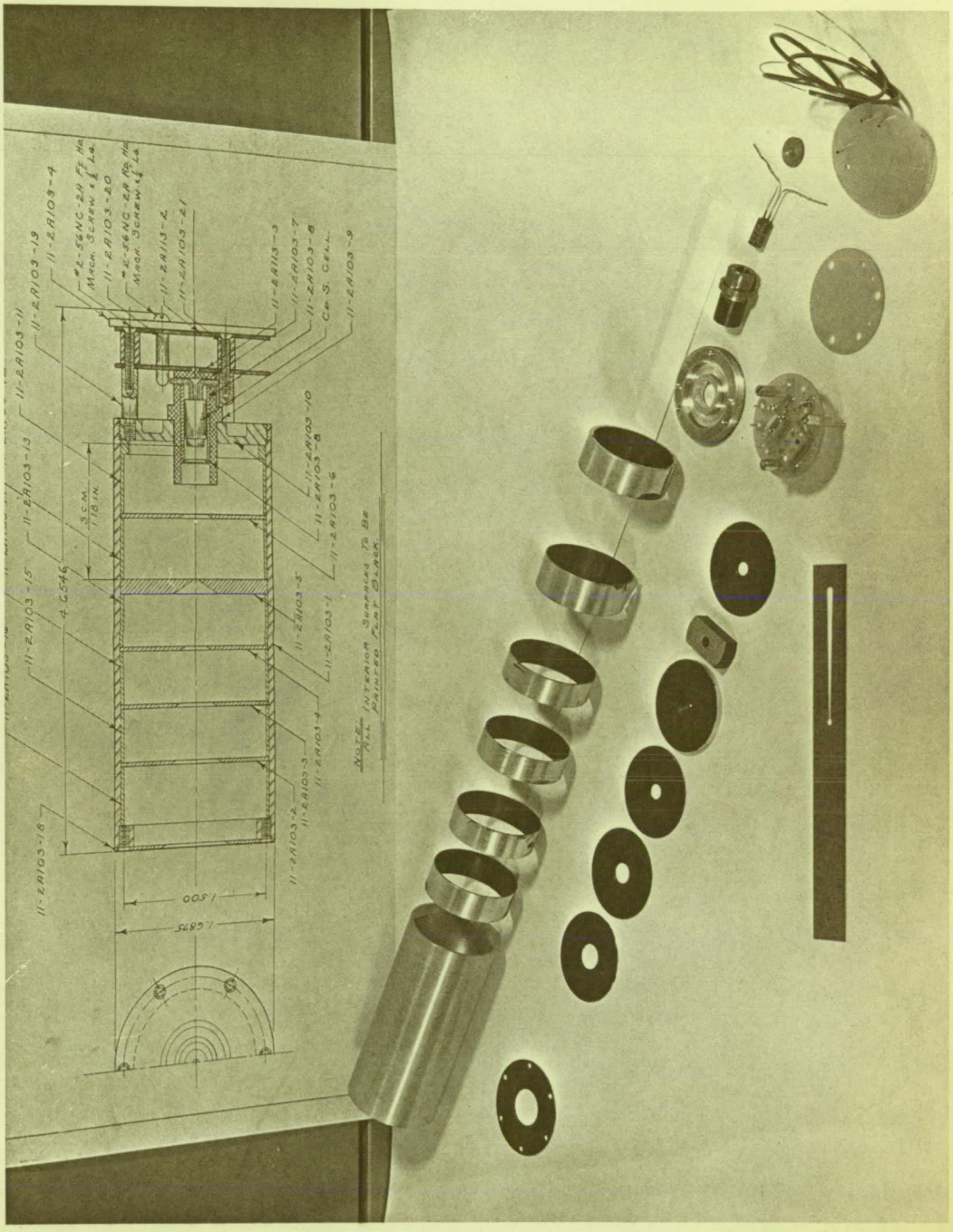
11-2A103-19
11-2A103-4
#2-56NC-2A FH No
Mach. Screw x 1/2 Lg.
11-2A103-20
#2-56NC-2A RH No
Mach. Screw x 1/2 Lg.
11-2A113-2
11-2A103-21
11-2A113-3
11-2A103-7
11-2M103-8
Co 3. Cell
11-2A103-9
11-2A103-11
11-2A103-13
11-2A103-15
4.6546
3.5 M
1/8 IN
11-2A103-10
11-2M103-6
11-2A103-6
11-2A103-5
11-2A103-1
11-2A103-4
11-2A103-3
11-2A103-2
11-2A103-18
.500
.689
NOTE:
ALL INTERIOR SURFACES TO BE
PAINTED FLAT BLACK

Fig. 22